1978

Mathematical modeling of pulsed-ultrasound systems

Thomas Wayne Buckman
Iowa State University

Mathematical modeling of pulsed-ultrasound systems

by

Thomas Wayne Buckman

A Dissertation Submitted to the

Graduate Faculty in Partial Fulfillment of

The Requirements for the Degree of

DOCTOR OF PHILOSOPHY

Major: Electrical Engineering

Approved:

Signature was redacted for privacy.

In Charge of Major Work

Signature was redacted for privacy.

For the Major Department

Signature was redacted for privacy.

For the Graduate College

Iowa State University
Ames, Iowa

1978

TABLE OF CONTENTS

LIST OF SYMBOLS

a_i	material coordinates
B(p)	weighted function related to magnitude of incident wave
c	propagation velocity of pulse in lossless medium
c_g	propagation velocity of pulse in lossy medium
c_{ijkm}	elastic coefficients
d_{ij}	strain rate
F_i	body force
G(v)	amplifier gain as a function of voltage
h_i	nonmechanical energy flux
J	magnitude of Jacobian matrix
k	complex propagation constant
k'	magnitude of real component of k
k''	magnitude of imaginary component of k
n_j	outer normal to a closed surface
P(t)	output pulse from A-scan type receiver
Q	acoustic source strength
R	reflection coefficient
r(i,y,p,q)	distance from (i,y) transducer element to (p,q) reflector element
r_t	determines range of r
$\Delta S(p,q)$	differential surface area of (p,q) reflector element
T_i^n	stress vector on surface with outer normal n
T_{ij}	stress tensor
u	internal energy per unit volume

u_i	particle displacement
v_i	particle velocity
V_{oi}	magnitude of ith component of particle velocity
$V_I(p,q)$	magnitude of incident particle velocity at (p,q) reflector element
$V_o(p)$	magnitude of incident wave related to voltage output of transducer in receiver mode
$V_T(t)$	total output voltage of transducer due to reflected wave
v_n	normal component of velocity at a surface
w	complex radian frequency
w'	magnitude of real component of w
w"	magnitude of imaginary component of w
w_{ij}	rigid body rotation rate
x_i	spatial coordinates
$x_{1N}(p)$	distance from reflecting surface to plane of transducer at point p
x_T	maximum value of x_{1N} at time t
$\Delta x_2(p)$	projection of ΔS onto x_2 axis at point p
z	acoustic impedance
α	angle of incidence
α_{ij}	rigid body rotation
ε_{ij}	spatial strain tensor
γ_{NP}	angle between a line connecting the (i,y) transducer element to the (p,q) reflector element and the plane of symmetry

γ_{TP}	angle between x_1 axis and a projection of the line for γ_{NP} onto the plane of symmetry
γ	viscosity coefficient
ϕ	velocity potential at a point
$\tilde{\phi}$	complex representation of ϕ
ϕ_o	magnitude of $\tilde{\phi}$
$\tilde{\phi}_R$	velocity potential of reflected wave at a point
$\tilde{\phi}_T$	velocity potential of total reflected wave
λ, μ	Lamé constants
ρ	density

CHAPTER I. INTRODUCTION

The Need

The objective of this thesis is to systematically develop an analytical technique to simulate the operation of a pulsed ultrasound system incorporating an A-scan display. Such systems are currently finding widespread use in biomedical engineering applications as a noninvasive diagnostic tool.

It was while working on the design of a new instrument in this area that the author first became aware of the need for such an analysis technique. The need becomes more evident when one considers the nature of some of the problems encountered in designing such systems.

All A-scan ultrasound systems yield information in terms of the magnitude of, and the time delay associated with, reflected pulses. The time delay is the time required for a pulse to propagate to and from an acoustic discontinuity while the magnitude of the pulse is proportional to the "nature" of the discontinuity. For example, such discontinuities exist at the boundaries of dissimilar mediums such as fat and muscle or muscle and bone. This information is typically displayed on a cathode ray tube with the horizontal axis proportional to time and the vertical axis proportional to magnitude. The operator or designer of a system must then interpret this output in order to derive the information needed for the particular application. Herein lies the problem; a designer needs a priori knowledge of the A-scan that will be produced in a proposed

application to know how difficult it is to uniquely associate the return pulses with particular boundaries. A simple example in this area should suffice to make this point clear.

The author has been involved with the design of a pulsed ultrasound system to measure lateral curvature of the spine. The approach used called for a plot to be made of the location of each of the vertebra relative to a fixed point. It was thought that a distinctive A-scan would be produced whenever the ultrasonic transducer was located directly over a tall boney vertebral protrusion called the spinuous process. This signal was to be identified by an electronic sensing circuit which would signal the instrument that the transducer was presently located over the center of a vertebra. Thus, by making a two-dimensional plot of the location of the transducer at these times one would eventually produce a graph which would contain the necessary information pertaining to the lateral displacement of vertebrae relative to one another.

The feasibility of such an approach is primarily dependent on the ease with which the spinuous process can be identified with an A-scan presentation, and, at present, the feasibility studies would have to be experimental in nature. Questions pertaining to the particular choice of a transducer, amplifier gain characteristics and many more parameters have to be worked out experimentally because no simple analytical techniques are available to simulate the operation of the system.

The techniques developed in this work go a long way towards remedying this problem. They represent a viable way of modeling an A-scan pulsed ultrasound system when simple reflection is the primary source of

the returned signal. The model includes such practical considerations as lateral translation and small angular rotation of the source with respect to the reflecting surface and allows variation of the radiated field distribution as well as variation of amplifer gain characteristics. In its present form, it provides a computer generated A-scan plot as its final output and is cheaper and faster than conducting the studies experimentally.

The most formidable part of generating the A-scan output is concerned with predicting the characteristics of pulses reflected off a regular or irregularly shaped object. A review of the literature at this point reveals little that would be helpful in solving this problem.

Literature Review

Over the years a variety of people have been concerned with analytical predications of reflected pulses, for a variety of reasons. A completely general algorithm has not been developed and, in every case, the investigators have taken advantage of certain simplifying assumptions that are consistent with the nature of their problem. They do, however, have one thing in common. They are primarily interested in either the exact shape of the reflected pulses, or the spectral content of the reflected pulses. This differs from the problem being considered in that the exact shape of the signal is not important in an A-scan, only the magnitude and approximate duration of a pulse are relevant.

It should be pointed out that determining the exact shape of a reflected pulse is a considerably more difficult problem, in general, than merely determining its magnitude and approximate duration. Thus, existing

techniques, when applicable, prove to be far more involved computationally than desired. This topic will be discussed in the literature review section.

A. Freedman (1) appears to have been concerned with underwater target identification when he developed his reflection algorithm for both continuous and pulsed waves. The technique requires the determination of discontinuities in a function, defined by the rate of change of solid angle with respect to distance, and in its higher order spatial derivatives. He applied the technique successfully to certain simple shapes (2) but it would be very difficult to apply this technique to any surface not easily describable in functional form.

D. M. Johnson (3) was involved with ultrasonic spectroscopy problems when he developed his Fourier transform technique for point sources by transforming the summation formula derived by W. G. Neubauer (4) for continuous wave reflection problems. Although the techniques can be applied to a wide variety of reflectors it does not consider finite size sources and furthermore the author states that it would not be possible to do so using his techniques, except possibly for certain simple geometries. In addition, the technique, as it stands, is quite complex computationally.

The remainder of the reflection algorithms found in the literature are limited to consideration of pulses reflected off plane surfaces or off certain simple shapes such as spheres and cylinders and are not applicable to irregular geometries. Examples of work done with pulses reflecting off planes can be found in the works of Ivanov (5,6,7,8), who transformed the problem to an integration in the complex plane, or in the works of Abramowitz (9), Towne (10,11), Cron and Nuttall (12), or Duykers (13).

Pulses reflected off cylinders were considered by Friedlander (14,15) and Forghieri (16) while similar problems for a sphere were considered by Metsaveer (17), Rudgers (18) and Hickling (19,20). These investigators used a variety of approaches ranging from classical boundary value problem methods to integral transform techniques.

The literature review that was conducted has lead to the following conclusions: (1) with the possible exception of the works by Freedman and Johnson, none of the methods discussed can be used to solve the required pulse reflection problem and (2) these methods, if applicable, would be unacceptable simply because they would require more time and expense than the experimental approach of solving the design problems. Thus, it appears that a new method is called for, one that is optimized for the determination of the magnitude and duration of the reflected pulse and one that would be considerably cheaper and faster than existing techniques.

This thesis is primarily concerned with the development of a pulse reflection algorithm derived from fundamental principles. The development is made with a view towards its theoretical justification and with a view towards the elucidation of all the inherent assumptions made in arriving at the result. It is felt that engineering is, to a large degree, concerned with the intelligent application of mathematical models and thus it is prudent to make the prospective user of an algorithm familiar with all of the limitations imposed by the assumptions made in arriving at the result.

With these facts in mind, Chapter II is devoted to the discussion of the wave equations which will be used to described the propagation of an

acoustical pulse in different media. Chapter III deals with the development of the necessary solutions to the wave equations. Chapter IV is devoted to the derivation of a useful reflection integral while Chapter V deals with the development of a computer algorithm to solve the reflection integral. Chapter V also includes the results of certain experiments which were designed to test the validity of the approach. Finally, conclusions are drawn and recommendations for future work are made in Chapter VI.

In concluding this introductory chapter, it should be pointed out that the material has been developed and presented in a format that will hopefully be of maximum utility to workers in biomedical ultrasonics. Biomedical engineering is an interdisciplinary science that often requires its workers to solve problems in areas for which they have little formal training. Quite often, attempts to gain the necessary knowledge are frustrated by one's inability to find suitable tutorial material. For example, in studying material related to the theory of sound, most elementary presentations were too restrictive while the advanced presentations were more general than needed. Difficulty arises in deciding exactly what principles and techniques need to be thoroughly understood and then extracting this information from the general body of knowledge. Much of the work done in arriving at the results in this thesis was concerned with these types of problems. Thus, an attempt has been made to present some of the material in a tutorial fashion. Hopefully this thesis can, in addition to its other objectives, serve as a starting point to those

who wish to acquaint themselves with the aspects of acoustical theory which are most likely to be of use to them in addressing a wide variety of problems in biomedical ultrasonics.

CHAPTER II. FUNDAMENTAL EQUATIONS OF SOUND

The prime objective of this chapter is to develop the equations necessary to describe the propagation of sound in either fluids or solids. Such a development proceeds quite readily from three other equations which are obtained from the applications of the principles of conservation of mass, momentum and energy. The applications are made in a manner that will allow the concurrent development of the wave equations for both fluids and solids. This approach differs from most standard developments of these equations and was chosen in order to emphasize the concepts common to both and to simplify the mathematical transition from one type of medium to the other.

The common approach taken in developing a wave equation for fluids is to use conservation equations stated in terms of density, pressure and particle velocity to derive a wave equation for one of the latter two variables. In the case of solids, pressure must be replaced by stress and particle velocity by particle displacement. This leads to a wave equation for particle displacement. The development for solids is obviously more complicated than it is for fluids since pressure, a scalar quantity, has been replaced by a rank two tensor, stress. For this reason many authors choose to assume a stress-strain (i.e., particle displacement) relationship and a simplified form of the momentum equation as the starting point and proceed to develop their equations from these relationships.

In contrast, this chapter will present mathematical statements of the conservation equations in terms of stress, particle displacement, particle velocity and density. When stated in this form these equations can be

used to derive wave equations which can be applied to a wide variety of fluids and solids.

It should be noted, at this point, that the reader's attention is being directed towards fluids and solids because these are the two environments in which A-scan ultrasound systems are used. However, the development itself is not limited to these mediums. With a suitable substitution of certain constants, equations applicable to gases could also be derived and a wave equation valid for anisotropic media is also developed in the process of arriving at the final results.

In the interest of simplicity, references have been cited to justify some of the less important relationships. Within the chapter itself, only key concepts and equations will be stated and discussed.

Conservation Equations

To begin this discussion it is noted that the correct interpretation and application of the various equations is dependent upon a proper understanding of the coordinate system or systems used in arriving at a particular equation.

The situation is complicated because of the nature of the various descriptions needed. For example, one is sometimes interested in the velocity at a particular point in a body. One is not concerned with what particle is at that point, one only wants to know the velocity of whatever particle happens to occupy that space at some instant in time. The description of the velocity at every point inside the body as a function of time in such a case would be called a spatial description. On the other

hand the interest is sometimes in the velocity of a particular particle as a function of time and one is willing to follow the particle as it moves from point to point inside the body. A description of velocity, as a function of time, for every particle inside the body would be called, in this case, a material description.

Material and spatial descriptions

Picture a fixed Cartesian coordinate system with axes a_i, $i = 1, 2, 3$. At some reference time t_o, every point inside a body will be identified by a particular vector a_i. Now consider another Cartesian coordinate system with the same origin and with the same orientation as the first, with axes x_i, $i = 1, 2, 3$. At some arbitrary time t, a point initially at a_i will be located at x_i. Thus, at any time t each a_i can be associated with an x_i by the functional relationship

$$x_i = x_i(t, a_1, a_2, a_3) \tag{2.1}$$

This relationship, when evaluated at t_o, will yield the initial position of the point.

$$a_i = x_i(t_o, a_1, a_2, a_3) \tag{2.2}$$

If one fixes the material coordinates a_i in equation (2.1), then x_i denotes the time-dependent coordinates of the particular point initially at a_i. The coordinates of any particular point depend only on time, the value of a_i merely states which point is under consideration. Under those conditions the ordinary derivative with respect to time of x_i would define the velocity of a particular point.

$$v_i = \dot{x}_i = \frac{dx_i}{dt} = \left(\frac{\partial x_i}{\partial t}\right)_{a_1 a_2 a_3} \tag{2.3}$$

Since a particular particle is being considered, this is actually a partial derivative with a_1, a_2, a_3 held constant.

A point which always moves with the material is called a particle or material point. Lines or surfaces composed of particles are called material lines or surfaces. The material inside a closed material surface is called a body.

Another concept that is important in the developments which follow is the variation of a scalar field quantity with respect to time. The mathematical statement of this idea depends on whether one is interested in the time variation at a point (spatial derivative) or the time variation following a particle (material derivative). In most cases the scalar field quantity is described in spatial coordinates, therefore the spatial and material derivative will only be defined for a quantity described in this manner.

Let $F(t, x_1, x_2, x_3)$ be a general scalar field quantity, which is described in spatial coordinates. The spatial derivative of the function is simply the partial derivative of F with respect to time. In order to define the material derivative, x_i is no longer treated as independent but is related to the material coordinates by substituting equation (2.1) into F. To determine the variation of this function with respect to time, for a specific particle, one fixes the value of a_i and applies the chain rule to obtain, with the help of equation (2.3):

$$\dot{F} = \frac{dF}{dt} = \frac{\partial F}{\partial t} + v_i \frac{\partial F}{\partial x_i} \tag{2.4}$$

The expression $\partial F/\partial t$ is that part of the material derivative resulting from the change of F with respect to time at a fixed point, and $v_i \partial F/\partial x_i$ is the part resulting from the motion of the particle in a field F whose value varies from point to point. So far attention has been directed towards the variation of an arbitrary scalar field quantity with respect to time for a particular particle. In order to apply the principles of conservation of mass, momentum and energy, it will be necessary to talk about the time variation of a property of a body, which is defined by a surface composed of a collection of particles.

Consider a collection of particles defining a volume $V_o = V(t_o)$ at time t_o, which by virtue of equation (2.1) would occupy a different volume $V = V(t)$ at some later time t. Let $F(t, x_1, x_2, x_3)$ now be a scalar material property referred to a unit volume. Then

$$P(t) = \int_V F(t, x_1, x_2, x_3) dV \tag{2.5}$$

where

$$dV = dx_1 dx_2 dx_3$$

is a property of the body which can be evaluated at any time t. The easiest way to evaluate this integral, at a specific time t, is to transform the integral to an integration over the material coordinates.

$$P(t) = \int_{V_o} F(t, x_1(t, a_1, a_2, a_3), x_2(t, a_1, a_2, a_3), x_3(t, a_1, a_2, a_3)) \left| \frac{\partial(x_1, x_2, x_3)}{\partial(a_1, a_2, a_3)} \right| dV_o \tag{2.6}$$

where $dV_o = da_1 da_2 da_3$ and $\left|\frac{\partial(x_1,x_2,x_3)}{\partial(a_1,a_2,a_3)}\right| = J$ the Jacobian determinant.

Equation (2.6) is obtained from (2.5) by application of a theorem of vector integral calculus (21). The integral is now in a form that is ideally suited to the determination of the rate of change of a body property with respect to time. One can now apply Leibnitz's rule (21) to obtain:

$$\frac{dP(t)}{dt} = \frac{d}{dt}\int_v F(t,x_1,x_2,x_3)dV = \int_{v_o} \frac{\partial}{\partial t}\{F(t,x_1(t,a_1,a_2,a_3),\ldots)J\}dV_o \tag{2.7}$$

Performing the indicated partial differention by the chain rule yields

$$J(\frac{\partial F}{\partial t} + v_i \frac{\partial F}{\partial x_i}) + F\frac{\partial J}{\partial t} \tag{2.8}$$

or by substituting equation (2.4) the form

$$J\frac{dF}{dt} + F\frac{\partial J}{\partial t} \tag{2.9}$$

is obtained for (2.8). Equation (2.7) can now be transformed back to an integration over the spatial coordinates by using the inverse of the Jacobian (i.e., 1/J).

$$\frac{dP(t)}{dt} = \int_v (\frac{dF}{dt} + F(\frac{1}{J}\frac{\partial J}{\partial t}))dV \tag{2.10}$$

This integral can be put into a more useful form by using the following relationship (21):

$$\frac{1}{J}\frac{\partial J}{\partial t} = \frac{\partial v_i}{\partial x_i} \tag{2.11}$$

Upon substituting (2.11) into (2.10) the final form is obtained as

$$\frac{dP(t)}{dt} = \int_v (\frac{dF}{dt} + F\frac{\partial v_i}{\partial x_i})dV \tag{2.12}$$

Equation (2.12) gives one a convenient formula for determining the rate of change of a body property with respect to time for a material property per unit volume, defined in spatial coordinates.

This equation concludes the section on various material and spatial descriptions. The specific examples that have been considered will be very useful in developing the conservation equations and will allow a better understanding of their particular formulations.

Conservation of mass

A statement of the conservation of mass for an arbitrary body can be obtained with the use of equation (2.12) by substituting $F = \rho$, where ρ is mass per unit volume (i.e., density), and setting the integrand equal to zero. Noting that the integral is valid for a differential volume, one can obtain a differential formulation of the conservation of mass equation.

$$\frac{d\rho}{dt} + \rho \frac{\partial v_i}{\partial x_i} = 0 \tag{2.13}$$

An equation expressing the conservation of mass in this form is traditionally called a continuity equation.

The development of the previous section allows one to develop a physical interpretation of equation (2.13). The equation implies that regardless of the movement a differential volume may experience, its total mass must remain constant. This is an important idea when one attempts to talk about the conservation of momentum applied to a differential volume or a body of any size and shape. Since momentum is, classically, mass

times velocity, requiring that the continuity equation be satisfied for a differential volume allows mass to be treated as a constant in expressing the momentum of that volume mathematically. This simplifies things considerably and is a necessary step in arriving at the classical wave equations.

Conservation of momentum

The equations which are often referred to as momentum equations are actually statements to the effect that the force acting on a body is equal to its time rate of change of momentum. This can be recognized as an application of Newton's second law. The application of this law to a differential volume is generally cited as a new axiom of continuum mechanics (22).

The development of this equation requires that one calculate the total force acting on a body and set this expression equal to the time rate of change of the momentum. The forces which act on a body are usually categorized as body forces, which are proportional to volume, and surface forces which are proportional to surface area. The only body force which will be considered is gravity, while the surface force will be characterized by a stress vector.

As a first step in deriving the momentum equation, the total surface force acting on a body will be considered.

Consider the example shown in Figure 1. Body A is stationary when force F_1 is applied. In order for the body to remain stationary a force F_2 must be applied. The total force and the cross-sectional area ΔA can

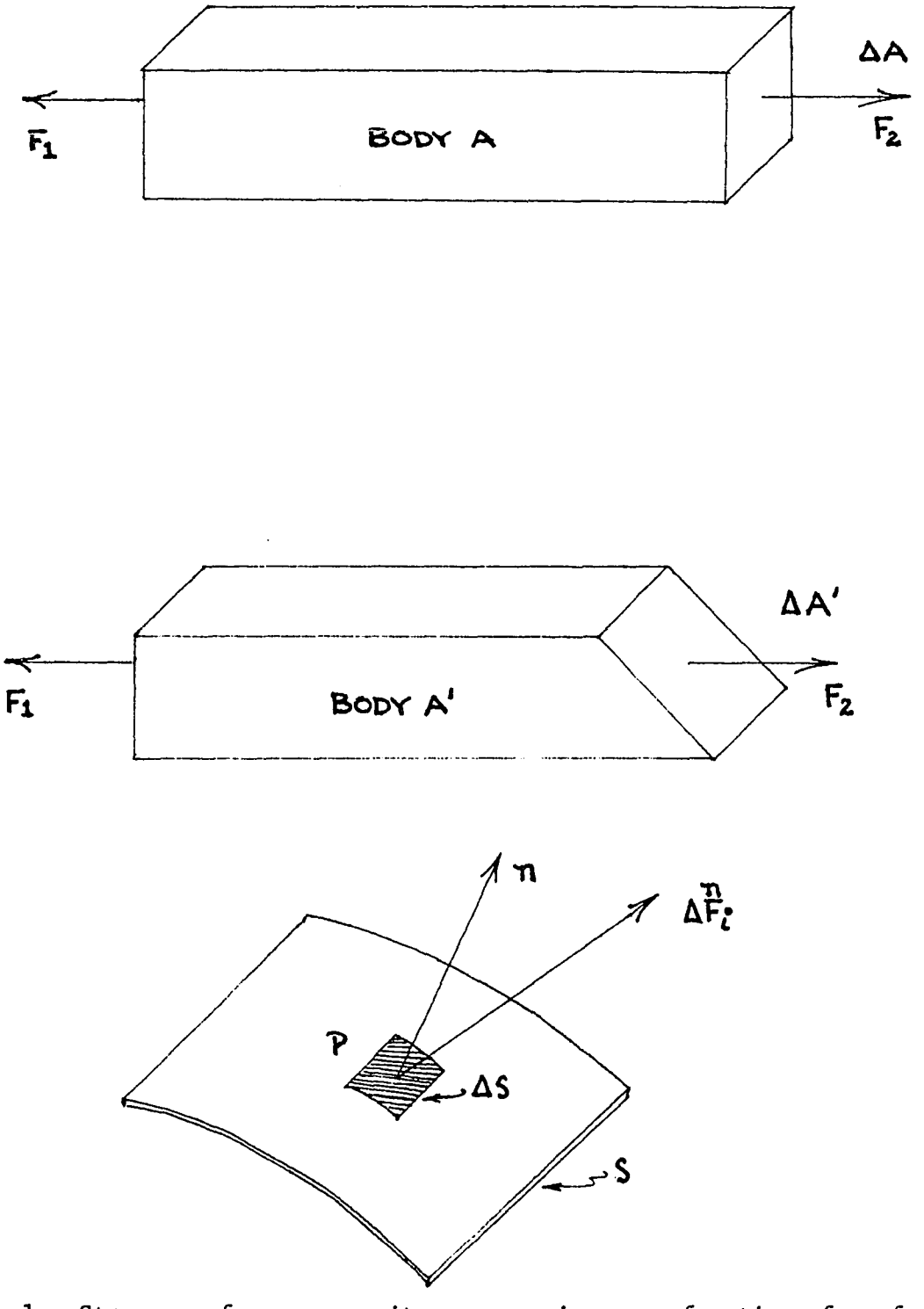

Figure 1. Stress or force per unit area varying as a function of surface orientation.

be used to define an average force per unit area applied at that end of the bar. This force per unit area, defined by F_2 divided by ΔA, is called stress. Notice that stress is a vector with magnitude and direction. Now, consider the same example after one end of the bar has been resectioned. This situation corresponds to body A' in Figure 1. It is obvious that even though the total force F_2 remains the same, the stress has decreased in magnitude, since $\Delta A'$ is larger than ΔA, and the direction of the stress vector relative to the normal of the surface has also changed. However, the total force applied has not changed. That is to say, when the stress is multiplied by the cross-sectional area the same total force, F_2, results in both cases.

This concept can now be generalized to arrive at a formal definition of stress. Let the surface S (Figure 1) represent an arbitrary internal or external surface in a body of material subjected to a system of loads. Over a small area ΔS of this surface in the neighborhood of point P, a system of forces acts which has a resulting $\overset{n}{\Delta F_i}$. The superscript n indicates that the total force acting on that differential area is a function of the orientation of the surface. The orientation is represented by the outer normal to the surface evaluated at the point P. And of course, in the general case, the value of $\overset{n}{\Delta F_i}$ is also a function of the location of point P in the body. It should also be noted that the direction of $\overset{n}{\Delta F_i}$ does not necessarily correspond to the direction of the outer normal n. The stress vector can now be formally defined as the limiting value of $\overset{n}{\Delta F_i}$ divided by ΔS as ΔS approaches zero.

$$\overset{n}{T_i} = \lim_{\Delta S \to 0} \frac{\overset{n}{\Delta F_i}}{\Delta S} \tag{2.14}$$

The total surface force acting on a body can now be computed by summing the surface forces on each differential volume in the body. When the body is in equilibrium the surface forces on all surfaces common to two volumes add to zero, so that one only needs to consider the surface forces on the surface bounding the body. This idea can be expressed in equation form as follows:

$$\text{Total surface force} = \oint_S \overset{n}{T_i} ds \tag{2.15}$$

Equation (2.15) is a somewhat unusual surface integral to evaluate in that the function to be integrated is a function of the outer normal of the surface on which it is being evaluated. In due course a form of equation (2.15) will be presented which is more practical for evaluation purposes.

The body forces due to gravity are somewhat simpler to evaluate. Defining the vector F_i as a body force per unit volume, the total body force acting on a body is

$$\text{Total body force} = \int_v F_i dv \tag{2.16}$$

The sum of these two force expressions must now be set equal to the time rate of change of the momentum. The momentum of a differential volume is $\rho v_i dv$ which is the momentum per unit volume. Thus the time rate of change of this quantity for the body is

$$\text{Time rate of change of momentum} = \frac{d}{dt} \int_v \rho v_i dv \tag{2.17}$$

Equation (2.12) can be applied to (2.17), which results in the following relationship, when it is assumed that the continuity equation is satisfied.

$$\frac{d}{dt}\int_v \rho v_i dv = \int_v \rho \frac{dv_i}{dt}\, dv \tag{2.18}$$

This leads immediately to an integral form of the momentum equation.

$$\int_v F_i dv + \oint_s \overset{n}{T}_i ds = \int_v \rho \dot{v}_i dv \tag{2.19}$$

In order to arrive at a differential form of the momentum equation the surface integral of the stress vector will now be modified to arrive at an equivalent volume integral. The stress vector can be related to a rank two tensor (23) by the following relationship

$$\overset{n}{T}_i = T_{ji} n_j \qquad i = 1, 2, 3 \tag{2.20}$$

The rank two tensor T_{ji} is commonly called the stress tensor, the stress components or simply the stress. It gives one a method of determining the stress vector at a point for a surface oriented in the n direction.

After substituting the right hand side of equation (2.20) into (2.19) one can transform the surface integral into a volume integral by use of the divergence theorem. This theorem expressed in summation convention is

$$\int_v B_{i,i} dv = \oint_s B_i n_i ds \tag{2.21}$$

where B_i is an arbitrary vector field. Thus, equation (2.19) becomes

$$\int_v (F_i + T_{ji,j} - \rho \dot{v}_i) dv = 0 \tag{2.22}$$

Since the integral holds for an arbitrary volume, the momentum equation in differential form is

$$\rho \dot{v}_i = F_i + T_{ji,j} \tag{2.23}$$

Notice that the density ρ appears in this equation as a constant. It can, however, vary from one differential volume to the next. Nevertheless, the particular development of the continuity equation given and the subsequent requirement that it be satisfied implies that the total mass associated with a differential volume remain constant as a function of time. It is only in this way that a meaningful definition of momentum can be arrived at, in the classical sense of the concept.

At this point there only remains the need for a conservation of energy equation to allow the subsequent derivation of the classic acoustic wave equations.

Conservation of energy

The conservation of energy equation will actually prove to be the necessary constitutive relationship that will characterize a particular medium. It leads to the classical stress-strain relationship for solids in addition to establishing a relationship between stress rate and particle velocity.

It can be envisioned at this point that one will eventually wish to talk about a source of sound waves creating a stress in a medium. The stress will in turn cause particles to be displaced in the medium. A stress displacement relationship could then form a basis for describing the dynamic disturbance caused by the source (i.e., the propagation of sound). If this is the case, and indeed it is, all forms of energy input to a differential volume will have to be assumed constant or zero in order

to establish a unique relationship between stress and particle displacement. This is the essence of the development which follows, and with these thoughts in mind a general energy equation will be stated and subsequently simplified to obtain the necessary relationships.

An energy balance written for a closed system can be stated as

rate of work by body forces	+	rate of work by surface forces	+	rate of energy increase due to nonmechanical energy flux	=	rate of increase of kinetic energy	+	rate of increase of internal energy

Since force per differential volume is $F_i dv$, the rate of work per unit volume is the rate of change with respect to time of force times distance or velocity times force

$$v_i F_i dv \tag{2.24}$$

In a similar fashion rate of work per unit area due to surface forces is

$$v_i T_{ji} n_j ds \tag{2.25}$$

For nonmechanical energy flux given by the vector h_i, the amount of energy entering per unit area is

$$-n_i h_i \tag{2.26}$$

where n_i is the unit outward normal.

Next it is noted that kinetic energy per unit mass is $\frac{1}{2} \rho v_i v_i$. The rate of change of this quantity with respect to time is

$$\frac{d}{dt} \int_v \frac{1}{2} \rho v_i^2 dv = \int_v (\rho v_i \dot{v}_i) dv \tag{2.27}$$

where the right hand side of equation (2.27) follows from equation (2.12), and the fact that

$$\frac{1}{2} \frac{d}{dt} (v_i^2) = v_i \dot{v}_i$$

Finally, if u equals internal energy per unit mass then ρu is internal energy per unit volume and the rate of change of this quantity with respect to time is by equation (2.12)

$$\frac{d}{dt}\int_v \rho u dv = \int_v \dot{\rho u} dv \tag{2.28}$$

Thus the energy equation can be expressed as

$$\int_v v_i F_i dv + \oint_s (v_i T_{ji} n_j - n_i h_i) ds = \int_v \rho(v_i \dot{v}_i + \dot{u}) \tag{2.29}$$

and by applying Green's theorem, equation (2.21), in conjunction with the fact that the integral must hold for an arbitrary volume, one obtains

$$v_i F_i + (v_i T_{ji})_{,j} - h_{i,i} = \rho(v_i \dot{v}_i + \dot{u}) \tag{2.30}$$

It is expedient, at this point, to reference the energy equation to a static state where it is assumed that the body forces are uniform and constant. In addition the nonmechanical energy flux is set equal to zero. With these assumptions the energy equation becomes

$$(v_i T_{ji})_{,j} = \rho v_i \dot{v}_i + \rho \dot{u} \tag{2.31}$$

where all of the terms are referenced to the static state. Upon expanding the left hand side

$$v_i T_{ji,j} + T_{ji} v_{i,j} = \rho v_i \dot{v}_i + \rho \dot{u} \tag{2.32}$$

and multiplying the momentum equation (2.23) by v_i, with the equation referenced to the static state, and substituting into (2.32)

$$T_{ji} v_{i,j} = \rho \dot{u} \tag{2.33}$$

The second order tensor $v_{i,j}$ can now be represented as the sum of a symmetrical and antisymmetrical tensor

$$v_{i,j} = d_{ij} + w_{ij} \tag{2.34}$$

where

$$d_{ij} = \frac{1}{2}(v_{i,j} + v_{j,i}) \qquad w_{ij} = \frac{1}{2}(v_{i,j} - v_{j,i})$$

The function d_{ij} is called strain rate while w_{ij} is descriptive of rigid body rotation of the differential volume. If one assumes that $w_{ij} = 0$ and $T_{ij} = T_{ji}$ then equation (2.33) becomes

$$T_{ij}d_{ij} = \rho\dot{u} \tag{2.35}$$

The assumption that $T_{ij} = T_{ji}$ can be shown to be true providing that all torques are moments of forces and all angular momenta are moments of linear momenta (23).

In concluding this first major section of the chapter, it is helpful to state the two key equations of the section in the form in which they will be used. The first is the momentum equation (2.23) referenced to a static state

$$\rho\dot{v}_i = T_{ji,j} \tag{2.36}$$

and the second is the energy equation

$$T_{ij}d_{ij} = \rho\dot{u} \tag{2.37}$$

These two equations form the heart of the wave equation derivations in the next section.

Acoustic Wave Equations

It is apparent at this point that equations (2.36) and (2.37) cannot be used in their present form to produce one equation with an unknown, such as the wave equation. The problem is, of course, one too many varia-

bles. Thus it follows that one of the three variables must be related to one of the other two.

It was stated earlier that knowledge of stress and particle velocity would form the basis of discussing sound propagation. Therefore, the internal energy term must, in some sense of the word, be related to particle displacement or its time derivative particle velocity. The relationship that is needed is the classical stress-strain relationship which is derivable from the energy equation.

This relationship is often referred to as a differential statement of Hooke's Law. Hooke's Law states that a spring stretched a small distance by an applied force will produce potential energy in the form of a restoring force. The magnitude of the force is proportional to a constant which describes the stiffness of the spring. The stress-strain equation has an analogous interpretation in that a particle displaced by a stress will tend to return to its original position upon removal of that stress.

Thus the concept of strain, which is related to particle displacement, will be formalized in the next section as a necessary prelude to deriving the wave equation.

Stress-strain relationship

The term strain refers to a change in the relative positions of the material points in a body. If a particle located at the position x_i at time t was located at the position a_i initially, then the change in its relative position can be stated as $u_i = x_i - a_i$, which is the displacement vector. A differential approximation to the change in the relative displacement of two particles, assuming small displacement gradients, would

then be stated as

$$du_i = \frac{\partial u_i}{\partial x_j} dx_j \tag{2.38}$$

The second-order tensor $\partial u_i/\partial x_j$ can be separated into symmetrical and antisymmetrical tensors ε_{jk}, α_{jk} giving

$$du_i = (\varepsilon_{ij} + \alpha_{ij})dx_j \tag{2.39}$$

where

$$\varepsilon_{ij} = \frac{1}{2}\left(\frac{\partial u_i}{\partial x_j} + \frac{\partial u_j}{\partial x_i}\right) \text{ and } \alpha_{ij} = \frac{1}{2}\left(\frac{\partial u_i}{\partial x_j} - \frac{\partial u_j}{\partial x_i}\right) \tag{2.40}$$

The tensor α_{ij} describes the rigid body rotation, whichhas been assumed to be zero, giving

$$du_i = \varepsilon_{ij} dx_j \tag{2.41}$$

where ε_{ij} is called the spatial strain tensor.

If one defines the strain rate as the derivative with respect to time of the strain one obtains

$$\dot{\varepsilon}_{ij} = \frac{1}{2}(v_{i,j} + v_{j,i}) = d_{ij} \tag{2.42}$$

the previously defined strain rate tensor.

The internal energy will now be defined as a function of strain only. If strain is designated as an independent thermodynamic variable, then by Gibbs' free-phase rule applied to a single-phase single-component system there is one other thermodynamic variable that is being treated as a constant. This variable could be, for example, temperature or entropy to name but a few. The choice is dictated by the desired application of the resulting equations. In some cases an isothermal condition might be a realistic assumption while in others constant entropy might be better.

The choice makes no difference in the form of the wave equations, it only dictates under what conditions certain constants are evaluated.

With u defined as a function of strain, the time rate of change of internal energy is

$$\dot{u} = \frac{\partial u}{\partial \varepsilon_{ij}} \dot{\varepsilon}_{ij} \tag{2.43}$$

and substituting (2.42) and (2.43) into (2.37) gives

$$T_{ij} = \rho \frac{\partial u}{\partial \varepsilon_{ij}} \tag{2.44}$$

and an additional differentiation with respect to strain yields

$$\frac{\partial T_{ij}}{\partial \varepsilon_{km}} = \rho_o \frac{\partial^2 u}{\partial \varepsilon_{ij} \partial \varepsilon_{km}} \tag{2.45}$$

The standard assumption of the variation in density with respect to strain being negligible has been made and the density ρ is approximated by ρ_o, a constant. Assuming that the rate of change of stress with respect to strain is a constant

$$\frac{\partial T_{ij}}{\partial \varepsilon_{km}} = c_{ijkm} = \rho_o \frac{\partial^2 u}{\partial \varepsilon_{ij} \partial \varepsilon_{km}} \tag{2.46}$$

and for small displacements

$$T_{ij} = c_{ijkm} \varepsilon_{km} \tag{2.47}$$

The components of the rank four tensor c_{ijkm} are commonly referred to as the elastic coefficients.

Equation (2.36) can be combined with equation (2.47) to develop a general wave equation for elastic solids in terms of particle displacement as follows:

$$T_{ji,j} = \frac{c_{jikm}}{2} (u_{k,mj} + u_{m,kj}) \tag{2.48}$$

and substituting into equation (2.36)

$$\rho \dot{v}_i = \frac{c_{jikm}}{2} (u_{k,mj} + u_{m,kj}) \tag{2.49}$$

Noting that $\dot{v}_i = \ddot{u}_i$ and that $c_{jikm} = c_{jimk}$, which is a consequence of the symmetry of the strain tensor

$$\rho \ddot{u}_i = c_{ijkm} u_{k,mj} \tag{2.50}$$

which is the general wave equation for elastic solids.

As mentioned before, a separate wave equation for nonviscous fluids is required. This is necessary because strain is not a meaningful concept in a medium which cannot support strain. That is to say, the application of a stress to a nonviscous fluid does not result in a static deformation of that body which can be related to a change in its internal energy but rather it would result in a translation of that body which would be reflected in a potential or kinetic energy term. Even though strain itself is not a meaningful concept strain rate is a concept with some utility, as shown in the subsequent development.

From equation (2.42) and the determination of the time derivative of equation (2.47)

$$\dot{T}_{ji} = c_{jikm} \dot{\varepsilon}_{km} = \frac{c_{jikm}}{2} (v_{k,m} + v_{m,k}) \tag{2.51}$$

it follows then that

$$\dot{T}_{ji,j} = \frac{c_{jikm}}{2} (v_{k,mj} + v_{m,kj}) \tag{2.52}$$

and noting that $c_{ijkm} = c_{jimk}$

$$\dot{T}_{ji,j} = c_{jikm} v_{k,mj} \tag{2.53}$$

combining equation (2.53) and (2.36) leads to

$$\rho \ddot{v}_i = c_{jikm} v_{k,mj} \tag{2.54}$$

Equation (2.54) is a general wave equation in terms of particle velocity instead of particle displacement, and although it is being developed here for use in nonviscous fluids, it is in no way limited in its application to that medium alone.

A point of clarification is in order with respect to the use of the tensor c_{jikm} in a nonviscous fluid. In the sense that c_{jikm} is referred to as an elastic coefficient, the use of the symbol is objectionable because nonviscous fluids possess no elastic properties. However, in the sense that c_{ijkm} is a constant of proportionality and a first order approximation to the relationship between strain rate and stress rate the use of the symbol is entirely appropriate.

Equations (2.50) and (2.54) are in useful formats if the medium under consideration displays anisotropic characteristics. However, if one is dealing with an isotropic medium a considerable simplification of both equations can be made. The elastic coefficients for an isotropic solid can be stated as follows (24):

$$c_{ijkm} = (\lambda \delta_{ij} \delta_{km} + \mu \delta_{ik} \delta_{jm} + \mu \delta_{im} \delta_{jk}) \tag{2.55}$$

Substitution of this expression into equation (2.54) yields

$$\rho \ddot{v}_i = (\lambda + \mu) v_{k,ik} + (\mu)\, v_{i,mm} \tag{2.56}$$

and using the identity

$$v_{k,ik} = v_{i,kk} + \varepsilon_{ikl} \varepsilon_{lrs} v_{s,rk} \tag{2.57}$$

equation (2.56) becomes

$$\rho\ddot{v}_i = (\lambda + 2\mu)v_{i,kk} + (\lambda + \mu)\varepsilon_{ikl}\varepsilon_{lrs}v_{s,rk} \tag{2.58}$$

Using the Helmholtz theorem (23), any piecewise differentiable vector field can be expressed as the sum of two vector fields, one of which is solenoidal and the other irrotational. Thus,

$$v_i = v_i^s + v_i^p \tag{2.59}$$

where

$$v_{i,kk}^s = 0 \qquad \varepsilon_{lrs}v_{s,r}^p = 0 \tag{2.60}$$

If one limits the wave equation to irrotational fields then equation (2.58) reduces to

$$\rho\ddot{v}_i^p = (\lambda + 2\mu)v_{i,kk}^p \tag{2.61}$$

In the interest of notational simplicity the superscript p will be dropped, but it should be understood that all future references to wave equations will be made with the understanding that the disturbance is irrotational.

A parallel development could now be made for equation (2.50) which yields

$$\rho\ddot{u}_i = (\lambda + 2\mu)u_{i,kk} \tag{2.62}$$

this being the wave equation which will be applied to elastic isotropic solids. Equation (2.61) will, with one additional simplification, be applied to nonviscous fluids.

The coefficients λ and μ are called Lamé constants (23), μ also being called the shear modulus. Since a nonviscous fluid would have a zero

shear modulus, equation (2.61) becomes

$$\rho\ddot{v}_i = \lambda v_{i,kk} \tag{2.63}$$

which will be the wave equation used for nonviscous fluids.

The two wave equations, (2.62) and (2.63), form the basis of all future wave propagation analysis. It has been stated that they are valid for nonviscous fluids and elastic solids. For instance, when one states that a solid is elastic, that is simply another way of saying that all of the assumptions made in arriving at equation (2.62) can be satisfied by the particular solid being considered. A similar idea applies to fluids. Thus all future analysis presupposes that the material being considered can be adequately modeled by one of these two mathematical characterizations.

The most important restriction that this approach puts on a material is that it not absorb any energy from a wave propagating through it. That is to say the two models presented represent lossless materials; no mechanism for loss of energy was considered. However, classical acoustic theory does allow the introduction of a simple model for loss called viscosity and it is possible to develop wave equations for a viscous fluid as well as a viscoelastic solid. The mathematical development of the wave equation for viscous mediums represents a modest extention of the derivations presented in this chapter. Therefore, its statement will be deferred to Chapter III along with discussions of the solution of wave equations in lossless and lossy materials.

CHAPTER III. SOLUTIONS OF THE WAVE EQUATIONS

The main objective of this chapter is to determine a solution of the wave equation which can be used to describe the propagation of a pulse associated with a pulsed-ultrasound system. In addition, the behavior of the pulse when propagating in a lossless or lossy medium will be investigated by substituting the previously derived solution into an appropriate wave equation. Such an investigation has two objectives: (1) to verify that the descriptive physics agrees with physical observations of real systems and (2) to determine if there are any implicit mathematical limitations associated with the solution.

Determination of the General Solution

Experimental investigation of pulsed ultrasound systems reveals that the wave that is produced by the transducer and propagated in the medium is approximately an exponentially damped sinusoid. It is not important to this investigation to know how this pulse is produced, one only needs to accept the idea that the pulse is established as a function of time at the boundary between transducer and medium. A mathematical statement of this idea would be in the form of an initial-boundary value problem.

In the interest of simplicity, the problem will initially be stated in a general form which can be related to a single Cartesian component of either one of the two wave equations, (2.62) or (2.63). The wave equation in general form can be stated as follows:

$$U_{tt} - C^2 U_{xx} = 0 \qquad 0 < x < \infty;\ t > 0 \tag{3.1}$$

Notice that the equation with its limits identifies it as being analogous

to an infinite transmission line problem. Eventually, an additional boundary located a finite distance from the source will have to be considered. This boundary, along with its associated boundary conditions, will have to be related to the irregularly shaped object which reflects the incident pulse. The consideration of the effects of this boundary will be deferred to the next chapter. The problem that is presently being considered is the infinite transmission line problem. Its solution will eventually be used to describe the pulse that is incident on the reflecting boundary.

It is assumed that the system is initially at rest and thus the initial conditions for equation (3.1) are the following:

$$\text{I.C.} \quad U(x,0) = 0 \qquad U_t(x,0) = 0 \tag{3.2}$$

The boundary condition for equation (3.1) will be some function f(t) where the f(t) will be related to the pulse shape observed for pulsed-ultrasound systems.

$$\text{B.C.} \quad U(0,t) = f(t) \qquad t \geq 0 \tag{3.3}$$

The solution to this initial-boundary value problem is well-known (25) and has the following form.

$$U(x,t) = f(t - x/c) \qquad t - \frac{x}{c} \geq 0 \tag{3.4}$$

It can be seen from equation (3.4) the term x/c must have units of seconds for the argument of the function f to be dimensionally correct. This implies that c has units of velocity, which leads to the identification of the constant c as the propagation velocity of the function f. Thus equation (3.4) implies that this function will reproduce itself at values of $x > 0$, x/c seconds after the pulse is initiated at the boundary. In order

to apply these results to the problem at hand, the general f(t) will now be replaced with a specific piecewise function.

A reasonable representation of the pulses associated with pulse-ultrasound systems is given by equation (3.5).

$$U(0,t) = \begin{cases} U_o e^{-w''t}\cos w't & 0 < t < 10\pi/w'' \\ 0 & t > 10\pi/w'' \end{cases} \tag{3.5}$$

This leads to the solution for equation (3.1) given in the following equation.

$$U(x,t) = \begin{cases} U_o e^{-w''(t - \frac{x}{c})}\cos w'(t - \frac{x}{c}) & 0 < t - \frac{x}{c} < \frac{10\pi}{w''} \\ 0 & t - \frac{x}{c} > \frac{10\pi}{w''} \end{cases} \tag{3.6}$$

This solution can be put into a form which is easier to handle in future calculations by substituting

$$k' = \frac{w'}{c} \qquad k'' = \frac{w''}{c} \tag{3.7}$$

and noting that

$$U_o e^{-(w''t-k''x)}\cos(w't-k'x) = \mathrm{Re}\{U_o e^{-(w''t-k''x)} e^{j(w't-k'x)}\} \tag{3.8}$$

where Re{} stands for the real part of the complex function defined within the brackets. An additional simplification can be obtained by defining complex constants w and k in the following fashion.

$$w = w' + jw'' \qquad k = k' + jk'' \tag{3.9}$$

Thus, the final form of the solution given in equation (3.6) will be written as

$$\tilde{U}(x,t) = \begin{cases} U_o e^{j(wt-kx)} & \frac{x}{c} < t \leq \frac{10\pi}{w''} + \frac{x}{c} \\ 0 & t > \frac{10\pi}{w''} + \frac{x}{c} \end{cases} \tag{3.10}$$

where

$$U(x,t) = \mathrm{Re}\{\tilde{U}(x,t)\} \tag{3.11}$$

Graphical representations of this pulse are shown in Figure 2. Next, the validity of stating the solution in the form of equation (3.10) will be tested by direct substitution into a wave equation for lossless mediums.

Lossless Mediums

In view of equation (3.10) a solution for the ith component of the wave equation (2.62) can be stated as:

$$\tilde{U}_i = U_{io} e^{j(wt-kx_i)} \qquad \frac{x}{c} < t \leq \frac{10\pi}{w''} + \frac{x}{c} \tag{3.12}$$

Direct substitution of this solution into the wave equation yields

$$-\rho w^2 U_{io} e^{j(wt-kx_i)} = -(\lambda + 2\mu)k^2 U_{io} e^{j(wt-kx_i)} \tag{3.13}$$

which leads immediately to the following relationship.

$$\frac{w}{k} = \left(\frac{\lambda+2\mu}{\rho}\right)^{1/2} \tag{3.14}$$

The substitution of equations (3.9) and (3.7) into (3.14) results in equation (3.15).

$$c = \left(\frac{\lambda+2\mu}{\rho}\right)^{1/2} \tag{3.15}$$

This result is consistent with the interpretation that would be given to the term $(\lambda + 2\mu/\rho)$ by direct comparison of equation (2.62) with equation (3.1).

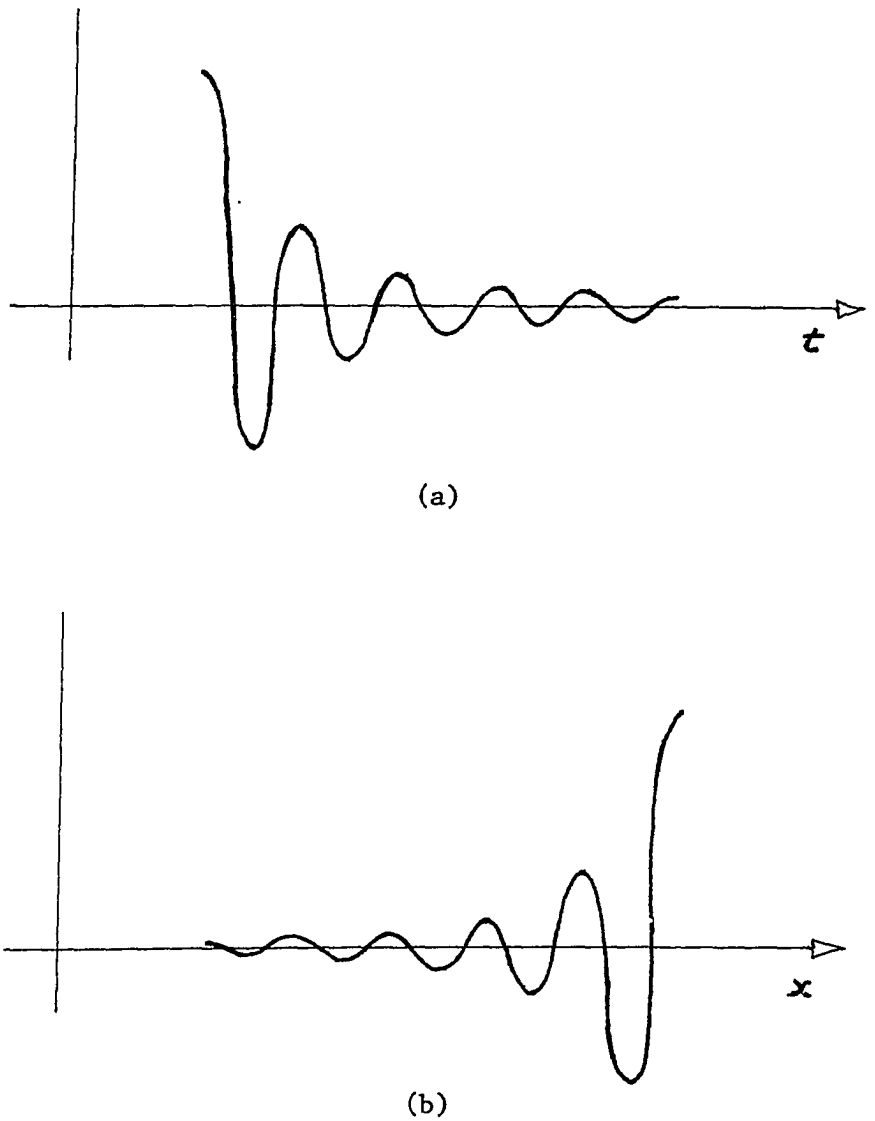

Figure 2. Exponentially damped sinusoidal pulse. (a) Propagating pulse as a function of time with position fixed. (b) Propagating pulse as a function of position with time fixed.

Finally, the validity of a solution in the form of equation (3.12) needs to be investigated for a lossy medium.

Lossy Medium

The investigation of pulses propagating in a viscous medium requires the derivation of a wave equation for viscous material. This is a relatively simple matter and can be accomplished by extending theory already presented in Chapter II.

Viscous effects are classically accounted for by introducing an additional term into the stress-strain relationship. Therefore, the Voigt model (26) for viscous materials will be introduced which regards stress to be a function of strain and strain rate. A statement of this model for isotropic viscoelastic material is

$$T_{ji} = (\lambda + 2\mu)u_{i,j} + \gamma\dot{u}_{i,j} \tag{3.16}$$

Differentiating (3.16) with respect to the jth index and substituting into equation (2.36) yields a wave equation for viscoelastic material as

$$\rho\ddot{u}_i = (\lambda + 2\mu)u_{i,jj} + \gamma\dot{u}_{i,jj} \tag{3.17}$$

If one substitutes a solution of the form given in equation (3.12) the the following analysis results:

$$-w^2\rho = -(\lambda + 2\mu)k^2 - j\lambda k^2 w$$

$$k^2 = \frac{\rho w^2}{(\lambda+2\mu)+jw\gamma}$$

$$k = w\left(\frac{\rho}{\lambda+2\mu}\right)^{1/2}\left(\frac{1}{1+jw\gamma/(\lambda+2\mu)}\right)^{1/2} \tag{3.18}$$

If one now approximates the expression on the far right of (3.18) by the

first two terms of a power series expansion then

$$k = w\left(\frac{\rho}{\lambda+2\mu}\right)^{1/2}\left(1 - j\,\frac{w\gamma}{2(\lambda+2\mu)}\right) \tag{3.19}$$

which is an acceptable approximation for $\frac{w\gamma}{(\lambda+2\mu)} << 1$. Once again letting $k = k' + jk''$ and noting that $\left(\frac{\lambda+2\mu}{\rho}\right)^{1/2} = c$ yields

$$k' + jk'' = \frac{w}{c} - j\,\frac{w^2\gamma}{2\rho c^3} \tag{3.20}$$

and again letting

$$w = w' + jw''$$

$$k' + jk'' = \frac{w'}{c} + j\,\frac{w''}{c} - j\,\frac{\gamma}{2\rho c^3}\left((w'^2 - w''^2) + j2w'w''\right) \tag{3.21}$$

or

$$k' + jk'' = \left(\frac{w'}{c} + \frac{w'w''\gamma}{\rho c^3}\right) - j\left(\frac{\gamma}{2\rho c^3}\left(w'^2 - w''^2\right) - \frac{w''}{c}\right)$$

and equating coefficients.

$$k' = w'\left(\frac{1}{c} + \frac{w''\gamma}{2\rho v^3}\right) \qquad k'' = \frac{-w'^2\gamma}{2\rho c^3} + w''\left(\frac{1}{c} + \frac{w''\gamma}{2\rho c^3}\right) \tag{3.22}$$

Now if one lets

$$\frac{1}{c_g} = \frac{1}{c}\left(1 + \frac{w''\gamma}{2\rho c^2}\right) \qquad \alpha = \frac{w^{12}\gamma}{2\rho c^3} \tag{3.23}$$

then

$$k' = \frac{w'}{c_g} \qquad k'' = -\alpha + \frac{w''}{c_g} \tag{3.24}$$

and one obtains, after expanding equation (3.12) and substituting the above relationships, equation (3.25).

$$\tilde{u}_i = Uo_i e^{-\alpha x_i} e^{-w''\left(t - \frac{x_i}{c_g}\right)} e^{jw'\left(t - \frac{x_i}{c_g}\right)} \qquad \frac{x}{c_g} < t \leq \frac{10\pi}{w''} + \frac{x}{c_g} \tag{3.25}$$

The form of equation (3.25) carries with it some interesting implications about pulses propagating in viscoelastic materials that bear a closer look.

To begin with, the solution describes an exponentially damped sinusoid propagating through the medium exactly as it did in the lossless case, except the amplitude now decreases exponentially with respect to propagation distance. In addition, the magnitude of the damping is proportional to the square of the frequency w', the natural frequency of the transmitted pulse. It is also interesting to note that the entire pulse now propagates at a different velocity than it did in the lossless case. Since all of the terms in equation (3.23) are positive, the implication is that the viscosity causes the pulse to propagate at a slower rate than before.

As interesting as these ideas are, it is not the purpose of this thesis to investigate their accuracy quantitatively. It is simply noted at this point that all of the implications made are reasonable from a qualitative standpoint. It should also be remembered that the primary purpose of the solution is to provide a reasonable representation of the propagation of the pulse to the reflecting surface. Once again, the implications of the previous two sections reveals nothing that poses an immediate problem. However, there is a limitation on the maximum amplitude of the pulse that needs to be considered which leads to a condition called the small-amplitude criterion.

Small-Amplitude Criterion

In the classical theory of time-harmonic acoustic fields, it is assumed that all variables have the same functional form (i.e., $e^{j(wt-kx_i)}$). It is this assumption that gives classic continuous wave mathematics most of its computational simplicity. However, it is this assumption which limits the magnitude of a signal that can be considered. This point can be aptly illustrated by considering the momentum equation, (2.36).

Suppose that one has knowledge of the particle velocity in a material and wishes to compute the stress gradient from the momentum equation. In order to do this the total time derivative of v_i must be calculated, which is

$$\dot{v}_i = \frac{\partial v_i}{\partial t} + v_i \frac{\partial v_i}{\partial x_i} \tag{3.26}$$

and assuming $\tilde{v}_i = Vo_i\, e^{j(wt-kx_i)}$ and substituting into (3.26) yield (3.27).

$$\dot{\tilde{v}}_i = jwVo_i e^{j(wt-kx_i)} - jkVo_i^2\, e^{j(2wt-2kx_i)} \tag{3.27}$$

The second term on the right hand side of (3.27) is a function of 2w instead of w and violates the assumptions previously made. Therefore, one requires that

$$kVo_i^2 << wVo_i$$

$$\frac{kVo_i}{w} << 1$$

and for real w and k

$$\frac{Vo_i}{c} << 1 \tag{3.28}$$

Thus, the basic criterion that is established to insure that all variables have the form $e^{j(wt-kx_i)}$ is that the magnitude of the particle velocity be much less than the magnitude of the propagation velocity. A wave that meets such a criterion is commonly referred to as a small amplitude wave. One also notes from the definition of particle displacement (i.e., $u_i = x_i - a_i$) that $v_i = \dot{u}_i$ and thus from equation (3.12), equation (3.28) can also be expressed as

$$\frac{wUo_i}{c} << 1 \tag{3.29}$$

Extending equation (3.29) to the case where w is complex in a lossless medium would yield

$$\frac{(w^{2'}+w^{2''})^{1/2}Uo_i}{c} << 1 \tag{3.30}$$

and for the lossy case

$$\frac{(w^{2'}+w^{2''})^{1/2}Uo_i}{c_g} << 1 \tag{3.31}$$

Equations (3.30) and (3.31) can now be used to establish a limit on the degree of exponential damping allowed in the pulse description since increasing the damping or shorting the duration of the pulse leads to increased particle velocity and in the lossy case to decreased propagation velocity, which quickly violates the small signal criterion.

The small signal criterion represents the most important restriction on the use of the solutions presented in this chapter. However, essen-

tially all diagnostic ultrasound devices use low intensity sound waves; this implies that the criterion should not prove to be excessively restrictive.

There are many additional speculations that could be raised concerning the application of the classic wave equation to certain materials that pulsed-ultrasound systems operate in. Human tissue is one example of such a material. Considerable amounts of research have been done in this area in the past and continue to be done in the present. However, as stated before, the prime objective of this analysis is to have an acceptable first order approximation of the propagation of a pulse to and from a reflecting surface. If the various constants that are used in the equations are carefully evaluated at suitable frequencies, the classic wave equations should provide a sufficiently accurate description.

Thus, the solutions presented in this chapter will now be used to describe the pulse incident upon an irregularly shaped boundary and, along with suitable boundary conditions, will be used to determine the characteristics of the reflected pulse. This determination is the subject of the material presented in the next chapter.

CHAPTER IV. REFLECTED PULSES

It has already been mentioned in the introductory chapter that reflected pulse problems have been considered in the literature for a number of years. It was also mentioned that the techniques used were basically one of two types, either a boundary value problem approach or an integral transform technique. Both methods are severely limited by the types of boundaries that can be handled computationally. Thus, a well-known method that gives approximate solutions to reflected wave problems has been adopted. The method is based on a branch of geometric optics called the theory of physical optics.

Physical optics is a technique of the theory of geometric optics. It is a technique which yields approximate solutions to certain types of boundary value problems. The accuracy of the solution is determined by how well a given problem can meet certain idealized conditions. These conditions will prove to have the greatest effect on limiting the types of problems that can be solved by the algorithm developed in this thesis.

The chapter will begin with a discussion on geometric optics as a prelude to a discussion on physical optics. Following this discussion, a surface integral will be developed which will be the heart of the mathematical model developed for pulse-ultrasound systems.

The discussion on geometric optics will begin by conceptually considering a wave striking the boundary between two dissimilar materials.

Geometric Optics

Observation of roughly equivalent situations in nature indicate that when a wave encounters a boundary or obstacle in its path a new wave emanates as if from the boundary itself. In the case of the boundary being infinite in extent, one would say that the wave was reflected or scattered and in the case where the boundary is reduced to a point, one would say that the wave was diffracted by the obstacle. Even if the boundary is not infinite, one continues to say that the wave is reflected providing that the extent of the boundary remains large with respect to the wavelength of the incident wave. In a similar way, the wave is viewed as being diffracted given that the extent of the boundary remains small with respect to the wavelength. In between these two regions a variety of curious phenomena can occur. In all fairness, it is not accurate to limit the concept of diffraction to small obstacles since the characteristic that identifies diffraction also arises when a wave strikes the edge of a plate for example, which in itself may be very large in extent.

Therefore, any large, noninfinite body can give rise to both reflected waves and diffracted waves, but if analysis is limited to the reflected waves one is dealing with the theory of geometric optics. In addition, the extent to which the theory of geometric optics can yield an approximation to the total solution of a problem is directly proportional to the extent to which the contributions of the diffracted waves can be neglected.

Within the theory of geometric optics there exists two main divisions which may be referred to as specular reflection and scattered reflection.

Scattered reflection arises when the surface is "rough" and the incident wave gives rise to a reflected wave at each point on the surface that emanates energy uniformly into a infinite halfspace; this is the inherent assumption of physical optics. The definition of what constitutes a rough surface will be addressed shortly and it is, as might be expected, a frequency dependent concept. Specular reflection on the other hand assumes a perfectly smooth surface with the incident wave being reflected at each point on the surface in a direction determined by Snell's law and it is assumed that this particular direction receives all of the reflected energy. This statement is true regardless of the frequency of the incident waveform for the case of a "perfectly" smooth reflector. However, a perfectly smooth surface appears not to exist and the definitions of specular and rough are relative concepts that are related to the frequency of the incident waveform and the dimensions of the irregularities of the surface.

The classical equation used to make this dichotomous decision is referred to as the Rayleigh criterion (27). Essentially it requires that one view two rays located a differential distance apart in space striking a boundary in such a way that one ray would strike the top of the irregularity while the other would strike a portion of the surface which would be viewed as the bottom of the irregularity. Now if it is assumed that the irregularities are h units high, then for the case where the incident rays are normal to the plane of the surface, one can define a path difference of 2h units. However, as the angle of incidence slowly increases from zero toward ninety degrees, the actual path difference between

the two rays tends toward zero. In equation form this can be expressed as

$$\Delta d = 2h\cos\phi_i \tag{4.1}$$

where ϕ_i is the angle of incidence which is equal to 0 at normal incidence, and Δd is the path difference. The path difference can now be expressed as a phase difference by

$$\Delta\theta = \frac{2\pi}{\lambda'}\Delta d = \frac{4\pi h}{\lambda'}\cos\phi_i \tag{4.2}$$

where λ' is the wavelength of the incident wave. A value of π radians for $\Delta\theta$ is viewed as producing maximum interference or scattering while a value of zero radians is viewed as producing no interference and hence specular reflection. The division between rough and smooth is then arbitrarily chosen as $\Delta\theta = \pi/2$. This value immediately leads to the Rayleigh criterion which is

$$h < \frac{\lambda'}{8\cos\phi_i} \tag{4.3}$$

Another way of viewing the Rayleigh criterion is to view the right side of equation (4.2) as a measure of roughness and say that the surface will only be considered smooth under one of two conditions.

$$\frac{h}{\lambda'} \to 0 \text{ or } \phi_i \to \pi/2 \tag{4.4}$$

Perhaps the greatest verification of the validity of the Rayleigh criterion is to be found in observations of natural events. An asphalt highway at high noon reflects light evenly in all directions whereas an individual driving west at sunset has often encountered specular reflection off of the same highway.

The key points that have been made or can be inferred from the last few paragraphs are the following: When one takes a physical optics approach to dealing with reflection it is assumed that the energy contained in an incident waveform is reflected uniformly in all directions (i.e., scattered by the surface). If one accepts the Rayleigh criterion as the definition of roughness then the only way that a surface can produce absolutely no scattering is for the frequency of the incident waveform to approach infinity since every surface is rough in some sense even if one has to view things on a microscopic level. If an irregularity on a plane surface becomes too large one would be forced to view the problem as reflection from an irregular boundary. And if a physical optics approach is used to deal with a reflection problem it would be possible to have regions on an irregular boundary, which according to the Rayleigh criterion should be viewed as regions of specular reflection and hence should not be included in a physical optics analysis. Contributions from these regions would be included via ray theory.

As can be inferred from the previous discussion, there are a number of classical methods that address themselves to waves incident on boundaries. Whether one chooses to use ray theory, physical optics or diffraction theory or a combination thereof is dictated by the assumptions that one can make about the boundary associated with a particular problem. In the case at hand, the physical optics approach will be found to be sufficient.

In the physical optics approach to solving reflection problems, each point on the reflecting surface is treated as if an infinite plane existed

at that point which is tangent to the surface at that location. The magnitude of the reflected wave is computed as the normal component of the reflected wave determined by the laws of specular reflection. Thus, in order to complete the discussion of geometric optics and pave the way for the development of the reflection integral, a development of the equations governing specular reflection for an infinite plane boundary will be presented.

Specular Reflection

When a transmitted wave strikes a boundary (i.e., incident wave) between two mediums at an arbitrary angle, boundary conditions require that one postulate the existence of both a reflected wave and a transmitted wave. In some special cases a phenomenon called mode conversion takes place and it is postulated that two types of reflected waves arise in addition to two types of transmitted waves. The existence of mode conversion is required in order to satisfy boundary conditions.

At a boundary between two fluids, for example, an incident wave gives rise to a single reflected and a single transmitted wave. At the boundary between two solids an incident wave gives rise to two reflected and two transmitted waves. The waves are referred to as reflected longitudinal and shear waves and transmitted longitudinal and shear waves. For instance, a wave function describing particle displacement would imply that particle displacement was normal to the axis of propagation if it was a shear wave or along the axis of propagation if it was a longitudinal wave. Longitudinal waves satisfy wave equations for irrotational fields

while shear waves satisfy wave equations for solenoidal fields. Since the waves produced by the sources to be considered later in this work are irrotational the discussion on reflected waves is limited to reflection of incident longitudinal waves.

Figure 3 represents an incident longitudinal wave striking a plane boundary between two mediums. Both mediums are treated as ideal lossless fluids. The expression for the incident particle velocity is

$$v_i^I = n_i^I v_i e^{jw(t-\frac{n_i^I x_i}{c_1})} \tag{4.5}$$

where $n_i^I = \sin\theta e(1) + \cos\theta e(2)$ with $e(i)$, $i = 1, 2, 3$ being unit vectors along the x_i, $i = 1, 2, 3$ axes while c_1 is the propagation velocity in medium one. The boundary conditions are 1) normal component of velocity is continuous across the boundary and 2) normal component of stress is continuous across the boundary. Normally, in the case of nonviscous fluids it is more common to talk about pressure than stress. The stress is related to the pressure, p, by

$$T_{ij} = -p\delta_{ij} \tag{4.6}$$

The off-diagonal components of the stress tensor are zero since a non-viscous fluid cannot support shear forces while the on-diagonal components are equal, in order to satisfy equilibrium requirements.

The boundary conditions can be satisfied by a transmitted and reflected wave of the form

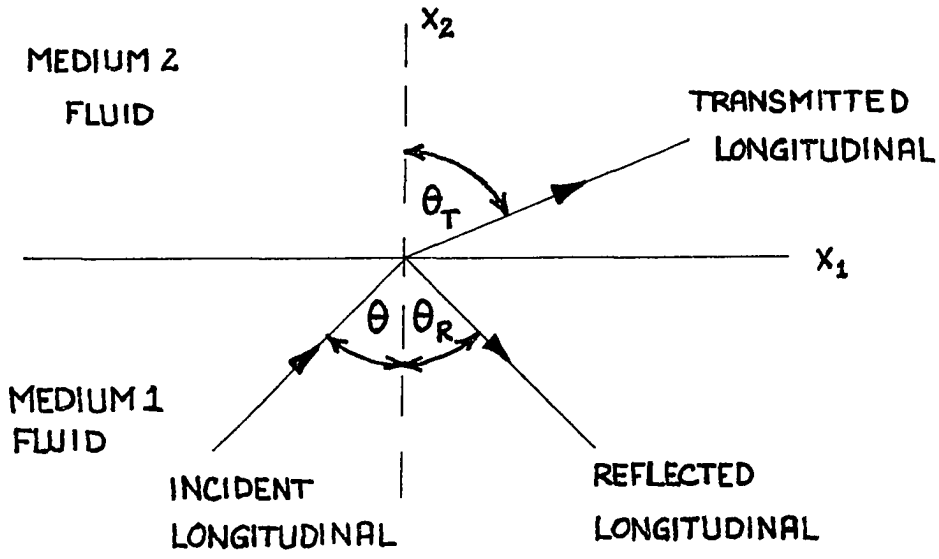

Figure 3. Plane wave incident on a fluid-fluid boundary.

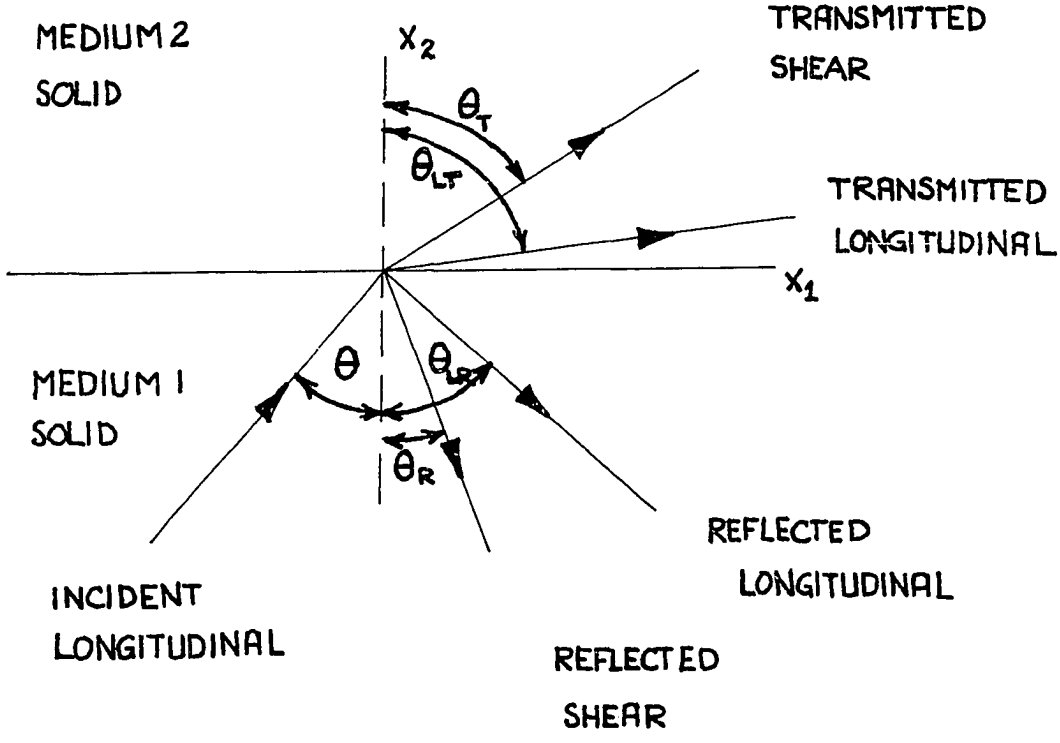

Figure 4. Plane wave incident on a solid-solid boundary.

$$v_i^T = n_i^T V_T e^{\frac{jw(t-n_i^T x_i)}{c_2}} \tag{4.6a}$$

$$v_i^R = n_i^R V_R e^{\frac{jw(t-n_i^R x_i)}{c_1}} \tag{4.6b}$$

where

$$n_i^T = \sin\theta_T e(1) + \cos\theta_T e(2) \tag{4.7a}$$

$$n_i^R = \sin\theta_R e(1) - \cos\theta_R e(2) \tag{4.7b}$$

In order to demonstrate this fact and to determine the relationship between magnitudes of incident and reflected waves the boundary conditions are stated in mathematical form as

$$e(2)\cdot(v_i^I + v_i^R - v_i^T) = 0 \tag{4.8a}$$

$$P_I + P_R - P_T = 0 \tag{4.8b}$$

The stress boundary condition has been restated simply as continuity of pressure. Using the equations (4.8b), (4.6b), (4.6a) and (4.5) now yields the following expression for continuity of velocity when evaluated at $x_2 = 0$

$$V_I\cos\theta e^{\frac{jw(t-x_1\sin\theta)}{c_1}} - V_R\cos\theta_R e^{\frac{jw(t-x_1\sin\theta_R)}{c_1}} = V_T\cos\theta_T e^{\frac{jw(t-x_1\sin\theta_T)}{c_2}} \tag{4.9}$$

To satisfy these conditions for all values of x_1 it is required that

$$\frac{\sin\theta}{c_1} = \frac{\sin\theta_R}{c_1} = \frac{\sin\theta_T}{c_2} \tag{4.10}$$

which is satisfied for

$$\theta = \theta_R$$

$$\frac{\sin\theta_R}{c_1} = \frac{\sin\theta_T}{c_2} \tag{4.11}$$

Equation (4.10) is the well-known Snell's law of geometric optics. Equation (4.11) implies that θ_T can only be real providing $\frac{c_2}{c_1}\sin\theta \leq 1$. If this condition is not satisfied total reflection occurs. Equation (4.9) now reduces to

$$V_I\cos\theta - V_R\cos\theta = V_T\cos\theta_T \tag{4.12}$$

This equation can now be combined with (4.8b) with the additional knowledge that

$$P_I = \rho_1 c_1 V_I,\ P_R = \rho_1 c_1 V_R,\ P_T = \rho_2 c_2 V_T \tag{4.13}$$

Equation (4.13) relates the magnitudes of velocity waves with the magnitude of the associated pressure wave and follows as a necessary inference from the momentum equation (2.36) and equations (4.5) and (4.6). Thus (4.8b) becomes

$$\rho_1 c_1 (V_I + V_R) = \rho_2 c_2 V_T \tag{4.14}$$

Assuming that $V_R = RV_I$, where R is called the reflection coefficient, (4.12) and (4.14) become

$$V_I\cos\theta(1 - R) = V_T\cos\theta_T \qquad \rho_1 c_1 (V_I + V_R) = \rho_2 c_2 V_T \tag{4.15}$$

Solving for R

$$R = \frac{z_2\cos\theta - z_1\cos\theta_T}{z_2\cos\theta + z_1\cos\theta_T} \tag{4.16}$$

where $z_2 = \rho_2 c_2$, $z_1 = \rho_1 c_1$ and the z's are called acoustic impedances.

The case of reflection from a solid-solid boundary, where mode conversion can take place, is considerably more complicated than the fluid-fluid boundary.

The boundary conditions are continuity of displacement and stress at the interface. For a wave at an arbitrary angle of incidence the wave will have both a normal and tangential or shear component, so the two boundary conditions produce four conditions that must be satisfied, continuity of the tangential and shear components of displacement and stress.

Referring to Figure 4 the incident wave is given by

$$u_i^I = n_i^I L_I \, e^{jw(t-\frac{n_i^I x_i}{c_{pl}})} \tag{4.17}$$

where $n_i = \sin\theta e(1) + \cos\theta e(2)$, while the transmitted and reflected longtudinal waves are

$$u_i^{LR} = l_i^R L_R \, e^{jw(t-\frac{l_i^R x_i}{c_{pl}})} \tag{4.18}$$

$$u_i^{LT} = l_i^T L_T \, e^{jw(t-\frac{l_i^T x_i}{c_{pl}})}$$

with

$$l_i^R = \sin\theta_{LR} \, e(1) - \cos\theta_{LR} \, e(2) \tag{4.19}$$

$$l_i^T = \sin\theta_{LT} \, e(1) + \cos\theta_{LT} \, e(2) \tag{4.20}$$

and the transmitted and reflected shear waves

$$u_i^{SR} = (\varepsilon_{ijk} e(3) n_k^R) S_R \, e^{\frac{jw(t - n_i^R x_i)}{c_1}} \tag{4.21}$$

$$u_i^{ST} = (-\varepsilon_{ijk} e(3) n_k^T) S_T \, e^{\frac{jw(t - n_i^T x_i)}{c_2}}$$

with

$$n_i^R = \sin\theta_R e(1) - \cos\theta_R e(2) \tag{4.22}$$

$$n_i^T = \sin\theta_T e(1) + \cos\theta_T e(2)$$

These equations can now be used in conjunction with the stated boundary conditions to yield the following matrix formulation for the various transmission and reflection coefficients (23).

$$\begin{vmatrix} \cos\theta_T & -\cos\theta_R & \sin\theta_{LT} & \sin\theta \\ \sin\theta_T & \sin\theta_R & -\cos\theta_{LT} & \cos\theta \\ z\sin 2\theta_T & \frac{-c_{p1}^2}{c_1^2} \sin 2\theta_R & f_2 & f_1 \\ z\cos 2\theta_T & \cos 2\theta_R & z\frac{c_2}{c_{p2}} \sin 2\theta_{LT} & \frac{-c_1}{c_{p1}} \sin 2\theta \end{vmatrix} \begin{vmatrix} t \\ r \\ T \\ R \end{vmatrix} = \begin{vmatrix} \sin\theta \\ -\cos\theta \\ f_1 \\ \frac{c_1}{c_{p1}} \sin 2\theta \end{vmatrix} \tag{4.23}$$

with

$$z = \frac{\rho_2 c_2}{\rho_1 c_1} \qquad f_1 = \frac{c_{p1}}{c_1} \left(1 - \frac{2c_1^2}{c_{p1}^2} \cos^2\theta\right)$$

$$f_2 = \frac{c_{p2}}{c_1} \left[1 - \frac{2c_2^2}{c_{p2}^2} \cos^2\theta_{LT}\right]$$

The coefficient of interest is R, the ratio of the magnitude of the reflected longitudinal wave to the incident longitudinal wave.

Finally, the case of a solid-liquid boundary needs special consideration, since a nonviscous fluid cannot support shear forces while a solid can. Therefore, the conditions on stress and displacement at the boundary are uncertain. The answer is not given by classical theory and it appears that the usual approach is to use the formula derived for the liquid-liquid boundary.

Thus, regardless of the application of the reflection integral either equation (4.16) or (4.23) will be used to determine the magnitude of the reflected wave arising at a boundary due to a known incident wave.

Reflection Integral

The material that has been presented thus far constitutes a suitable foundation for the consideration of the pulse reflection problem. The ability to predict the nature of pulses reflected off of irregularly shaped objects is just one aspect of modeling the operation of a pulsed-ultrasound system. However, it is the most formidable aspect of modeling such a system, and as such, it constitutes the heart of the entire model. The purpose of this section is to develop this key expression which will be referred to, henceforth, as the reflection integral.

The general nature of the problem being considered is one of a source radiating in the presence of a reflective object. Problems of this nature are common in acoustic fields. It is possible, in many cases, to formulate an expression for the "exact" solution to problems of this type, but an "exact" evaluation of the expression is often impractical. Therefore, it is common to see simplifications introduced in one of two ways. One of these is to consider a physical situation which is slightly different than

the original but is thought to behave in a similar manner. The object of such a consideration is to find a situation where a simpler expression for the solution can be formulated. The other approach is to put restrictions on ranges of values for certain variables that will allow the use of simplifying approximations.

Both of the techniques just mentioned will be used in arriving at the reflection integral; in addition, it will be advantageous to subdivide the reflection problem into a number of simpler problems which can be considered independently. In order to clarify the relationship between these simpler problems and establish the role of various approximations, a general discussion of the pulse reflection problem will be conducted before considering the mathematical details.

General considerations

The characteristics of a pulse reflected off an irregularly shaped object will be viewed as a function of two factors: (1) the description of the source field, and (2) the shape of the reflection boundary and the material characteristics of both the obstacle and the transmission medium. The general considerations begin with a discussion of the source field.

Conceptually, one seeks a mathematical description of the field radiated by the source when the obstacle is not present. This field will be defined as the incident field. The derivation of such a description can, in itself, be a complex problem. Typically, assumptions such as a point source or an incident uniform plane wave can be made in a reflection problem, but neither one of these will serve as an adequate description in

the case at hand. It can be observed experimentally, for example, that transducers of the same physical dimension and operating at the same frequency can generate different A-scans. Thus the radiation characteristic of a particular transducer is an important design parameter and needs to be included in a system model.

In view of the facts just mentioned, a simple laboratory technique was devised which would allow one to arrive at an empirically derived mathematical description of the incident field. The end result is to describe this field as a plane wave whose amplitude is allowed to vary from point to point on the wave front, has a shape identical to the pulse described in the previous chapter and propagates in a direction normal to the transducer (i.e., source) face. In addition, the description is defined only over an area of the same size and shape as the face of the transducer on a plane parallel to the wave front. The aspects of this description which are dependent upon the particular transducer being used are the area occupied by the wave front and the amplitude characteristics. In many ways the nature of the incident field is analogous to the radiation pattern of a flashlight.

It should be noted that the plane wave assumption is consistent with the idea that the acoustic beam (radiated field) has a constant area and shape on the wave front. That is, one is assuming negligible divergence of the beam which is approximately true only over a certain range of distances from the source. This idea is aptly illustrated with a flashlight. In many cases pulsed-ultrasound units are operated in such a range; thus, the assumption should not prove to be too restrictive. However, it should

be pointed out that the validity of the reflection integral will not be dependent on this assumption, it will merely reduce the final computational complexity.

Having determined an expression for the incident field, one now assumes that this expression can be used to determine values of the source field at the surface of the obstacle. This information, in conjunction with information on the shape of the boundary and nature of the material discontinuity, can be used to predict the characteristic of the reflected wave at the surface.

The description of the reflected wave at the boundary is an approximate one, based on an attempt to satisfy the necessary boundary conditions on a point-by-point basis. The essence of the technique is to assume an infinite plane tangent to a particular point on the surface and then calculate the value of the reflected wave at that point using the methods of the previous section. The validity of such an assumption, which is called the Kirchhoff approximation, has been investigated in a paper by W. C. Meecham (28), and he concludes that it is valid providing that the maximum slope of the surface at that point is much less than one and the propagation constant times the minimum radius of curvature is much greater than one. However, these restrictions where stated as being "reasonable" rather than absolute and they will not always be adhered to in this paper. Nevertheless, they do serve as an indicator of possible problem areas.

Once one has a description of the reflected wave on the surface of the obstacle, it is entirely appropriate to view the obstacle as a source

in its own right. For example, assume that the wave equation for particle velocity has been used to describe the incident wave, and that a description of the particle velocity of the reflected wave is now available at each point of the surface. It is just as easy to say that that particular pattern of particle velocity has been caused by a vibrating surface rather than a reflection. Thus, it is conceptually possible to reduce the original source-obstacle problem to an equivalent problem, where one seeks the radiation pattern of an "induced" source.

One rather obvious and intuitively attractive way to determine the radiation pattern of the source would be to model each differential surface element as a small source vibrating with the characteristic velocity found at that point. The total radiated field at any one point could then be computed as the vector sum of the contributions from each differential source. In the next part of this section, the mathematics involved with taking such an approach will be investigated.

Mathematical formulation

It will be assumed that a reasonably accurate determination of the reflected wave can be achieved by assuming that each point on the reflecting surface is acting as a simple point source in an infinite, rigid baffle. Obviously, the characteristics of a point source and an infinite rigid baffle need to be stated in order to formulate the reflection integral. This is most conveniently done in spherical coordinates. Therefore, vector differential operators and solutions to wave equations in spherical coordinates will be used for the present; this is in lieu of any attempt to maintain consistency with tensor notation.

In order to simplify the subsequent mathematics as much as possible, it is convenient at this point to introduce the idea of a velocity potential.

It can be recalled that the wave equations derived in Chapter II assumed an irrotational solution, that is, the curl of the resultant function is equal to zero. It is well-known that when the curl of a vector is zero, the vector can be represented as the gradient of a scalar function, which is often called a potential function. In virtually every case one can imagine it is easier to determine the potential function than it is the associated vector field quantity. Once the potential function is available the velocity is computed by an equation of the form given in (4.24).

$$\vec{V} = -\nabla\phi \tag{4.24}$$

In this equation ϕ represents the standard potential function of acoustics, the velocity potential, and $\vec{V}$ is the particle velocity.

It is not difficult to show by substitution and integration that the velocity potential is governed by an equation of the same form as the vector wave equations which govern particle velocity and particle displacement. The difference is that ϕ being a scalar results in a scalar wave equation rather than a vector wave equation. Thus, the governing equation for ϕ is

$$\nabla^2\phi = \frac{1}{c^2}\frac{\partial^2\phi}{\partial t^2} \tag{4.25}$$

where the variable c is still interpreted as the propagation velocity.

Equation (4.25), when evaluated in the spherical coordinate system, is in a convenient form to investigate the properties of a point source.

An acoustic point source is usually viewed as a small pulsating sphere that radiates energy uniformly in all directions. Therefore, the appropriate solution to the wave equation describes an outgoing spherical diverging wave that is only a function of r. Assuming that the sphere is radiating exponentially damped sinusoidal pulses, the solution is

$$\tilde{\phi} = \begin{cases} \frac{\phi_o}{r} e^{j(wt-kr)} & \frac{r}{c} - \frac{10\pi}{w''} \leq t \leq \frac{r}{c} \\ \\ 0 & t > \frac{r}{c} \end{cases} \tag{4.26}$$

where w and k are in general complex. (The development of (4.26) is analogous to the approach taken in arriving at equation (3.10).) A method is now needed to relate the magnitude of equation (4.26) to the local particle velocity found at that point. Once this is accomplished one can use the values of the particle velocity determined for the reflected wave at the surface to define a continuous array of point sources on the reflecting surface.

In acoustics, the "strength" of any source is defined as the amplitude of the scalar product of particle velocity and surface area, integrated over a closed surface (29). In equation form this can be written as

$$Q = \int_S v_n ds \tag{4.27}$$

where v_n is the amplitude of the particle velocity normal to the surface and Q is the source strength. For a point source, the velocity vector would be radially directed and everywhere normal to the surface of a

sphere. Thus, the velocity vector can be determined by differentiating the velocity potential in the r direction.

$$\frac{\partial \phi}{\partial r} = \frac{-\phi_o}{r^2} (1 + jkr) e^{j(wt-kr)} \tag{4.28}$$

Since kr is much less than one for a sphere approaching the size of a point, the particle velocity at the surface of the sphere is approximately,

$$\frac{\partial \phi}{\partial r} = \frac{-\phi_o}{r^2} e^{jwt} \tag{4.29}$$

This equation then leads to an expression for v_n

$$v_n = \frac{\phi_o}{r^2} \tag{4.30}$$

Upon integrating v_n over the surface of a sphere, the following relationship between source strength and ϕ_o results.

$$\phi_o = \frac{Q}{4\pi} \tag{4.31}$$

Finally, equation (4.26) can be expressed in the following form.

$$\tilde{\phi} = \begin{cases} \frac{Q}{4\pi r} e^{j(wt-kr)} & \frac{r}{c} \frac{-10\pi}{w''} \leq t \leq \frac{r}{c} \\ 0 & t > \frac{r}{c} \end{cases} \tag{4.32}$$

The expression given in equation (4.32) is for the velocity potential of a point source radiating in an infinite isotropic homogeneous medium. However, the hypothetical point sources of the reflected wave are radiating in the presence of a boundary. The effect of the boundary, as mentioned earlier, is taken into account by determining the velocity poten-

tial of a point source radiating on the surface of an infinite, rigid baffle. The strength of such a source can be determined by integrating over a hemisphere since the presence of the baffle limits the radiation pattern to a hemispherical shape. This leads to a factor of 2π in (4.31), thus for a surface point source the velocity potential is as follows:

$$\tilde{\phi} = \begin{cases} \frac{Q}{2\pi r} e^{j(wt-kr)} & \frac{r}{c} \leq t \leq \frac{10\pi}{w''} + \frac{r}{c} \\ 0 & t > \frac{10\pi}{w''} + \frac{r}{c} \end{cases} \tag{4.33}$$

The transition from equation (4.33) to the reflection integral can now be accomplished in a straight forward manner. This transition requires that each differential surface element be viewed as a point source radiating in the presence of an infinite, rigid baffle. An expression for the strength of a differential source follows immediately from equation (4.27).

$$dQ = v_n ds \tag{4.34}$$

Thus, the differential contribution to the velocity potential is

$$d\tilde{\phi}_R = \begin{cases} \frac{v_n}{2\pi r} e^{j(wt-kr)} ds & \frac{r}{c} \leq t \leq \frac{10\pi}{w''} + \frac{r}{c} \\ 0 & t > \frac{10\pi}{w''} + \frac{r}{c} \end{cases} \tag{4.35}$$

where v_n now indicates the amplitude of the normal component of particle velocity associated with the reflected wave. The subscript R indicates the reflected field. The total velocity potential for the reflected wave

can now be determined by integrating equation (4.35) over the surface.

$$\tilde{\phi}_R = \frac{1}{2\pi} \int_s \frac{v_n}{r} e^{j(wt-kr)} ds \tag{4.36}$$

It should be noted in equation (4.36) that the limits on the range of t have not been included. This has been done for the sake of notational simplicity, however the limits do apply and it should be assumed that they are implied in future expressions unless stated otherwise.

It is now possible to express $\tilde{\phi}_R$ in terms of the incident field expression by introduction of the relationship between incident and reflected particle velocities which was developed in the section on specular reflection. Referring to Figure 5, the magnitude of the particle velocity for the reflected wave can be expressed as

$$V_R = RV_I \tag{4.37}$$

and the normal component of V_R would be cosα times V_R.

$$v_n = RV_I \cos\alpha \tag{4.38}$$

Thus, the strength of the point source located at that differential surface element is

$$dQ = RV_I \cos\alpha ds \tag{4.39}$$

where α is the angle of incidence. This means that equation (4.36) can now be expressed as

$$\tilde{\phi}_R = \frac{1}{2\pi} \int_s \frac{RV_I}{r} e^{j(wt-kr)} \cos\alpha ds \tag{4.40}$$

The evaluation of the reflection integral, as given in equation (4.40), needs to be approached cautiously because of the implied limits on the values of t and r. Recall that the kernal of the integral is nonzero

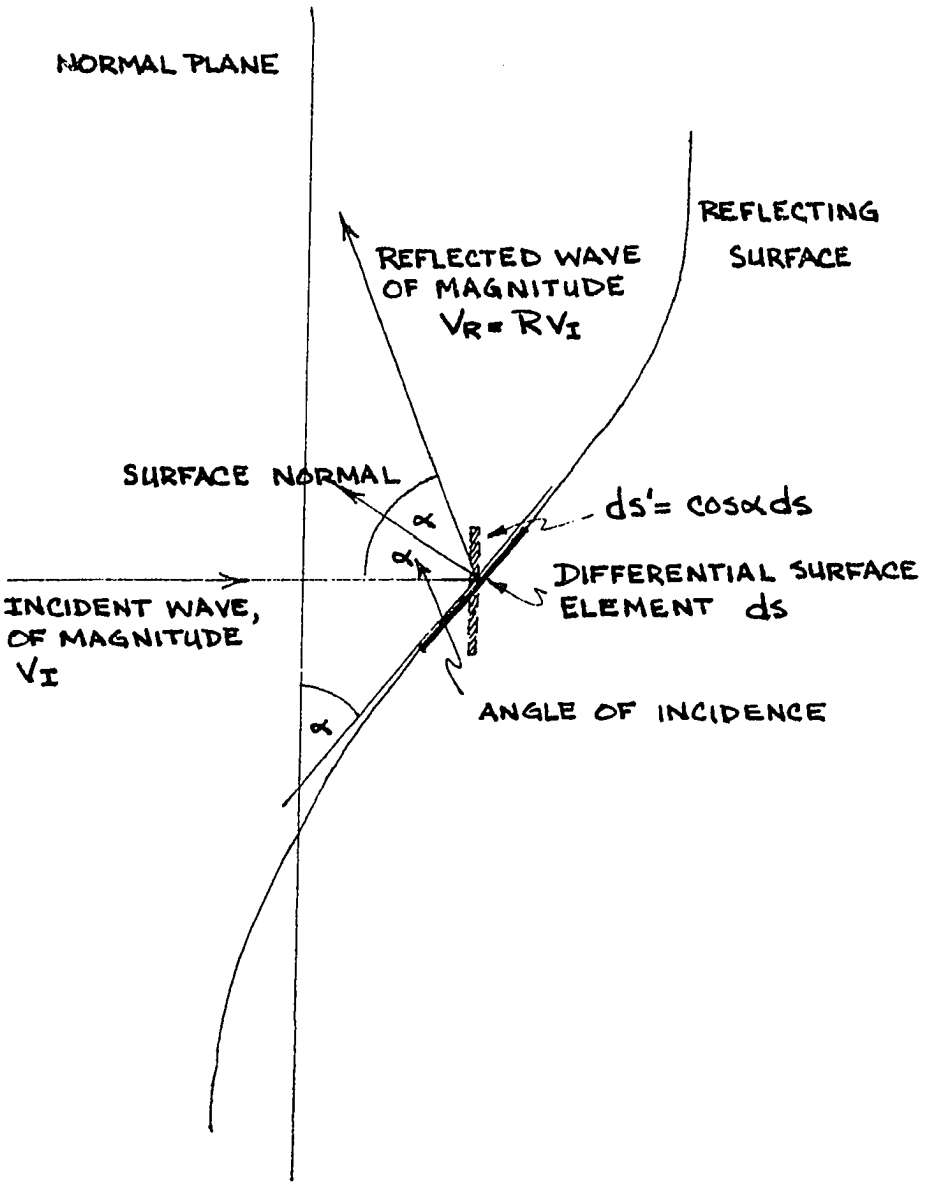

Figure 5. Plane wave reflected by a differential surface element.

only for the following values of t.

$$\frac{r}{c} \leq t \leq \frac{10\pi}{w''} + \frac{r}{c} \tag{4.41}$$

Now let

$$t = \frac{r_t}{c} \tag{4.42}$$

and substitute this into equation (4.41) which following minor manipulation of the inequality leads to the following limits on the value of r.

$$r_t - \frac{10\pi}{k''} \leq r \leq r_t \tag{4.43}$$

The implications of this unequality are illustrated in Figure 6. It implies at a particular value of t, only that portion of the reflecting surface between the spherical sheets s_1 and s_2 actually contribute to the velocity potential at point P. At a later instant in time it would be the portion of the surface between s_1' and s_2' that determines $\tilde{\phi}_R$ at point P. The reflection integral can now be restated as

$$\tilde{\phi}_R = \begin{cases} \frac{1}{2\pi} \int \frac{RV_I}{r} e^{jk(r_t - r)} \cos\alpha ds & r_t - \frac{10\pi}{k''} \leq r \leq r_t \\ 0 & r \geq r_t \end{cases} \tag{4.44}$$

where kr_t has been substituted for wt.

In the future, the expression given for $\tilde{\phi}_R$ in equation (4.44) will be referred to as a pulse reflection integral. This integral forms the basis of the summation formula developed in the next chapter to describe pulses reflected off irregular shaped objects when a finite size transmitter/receiver element is involved. It should be pointed out that the summation formula differs from the pulse reflection integral in that the integral

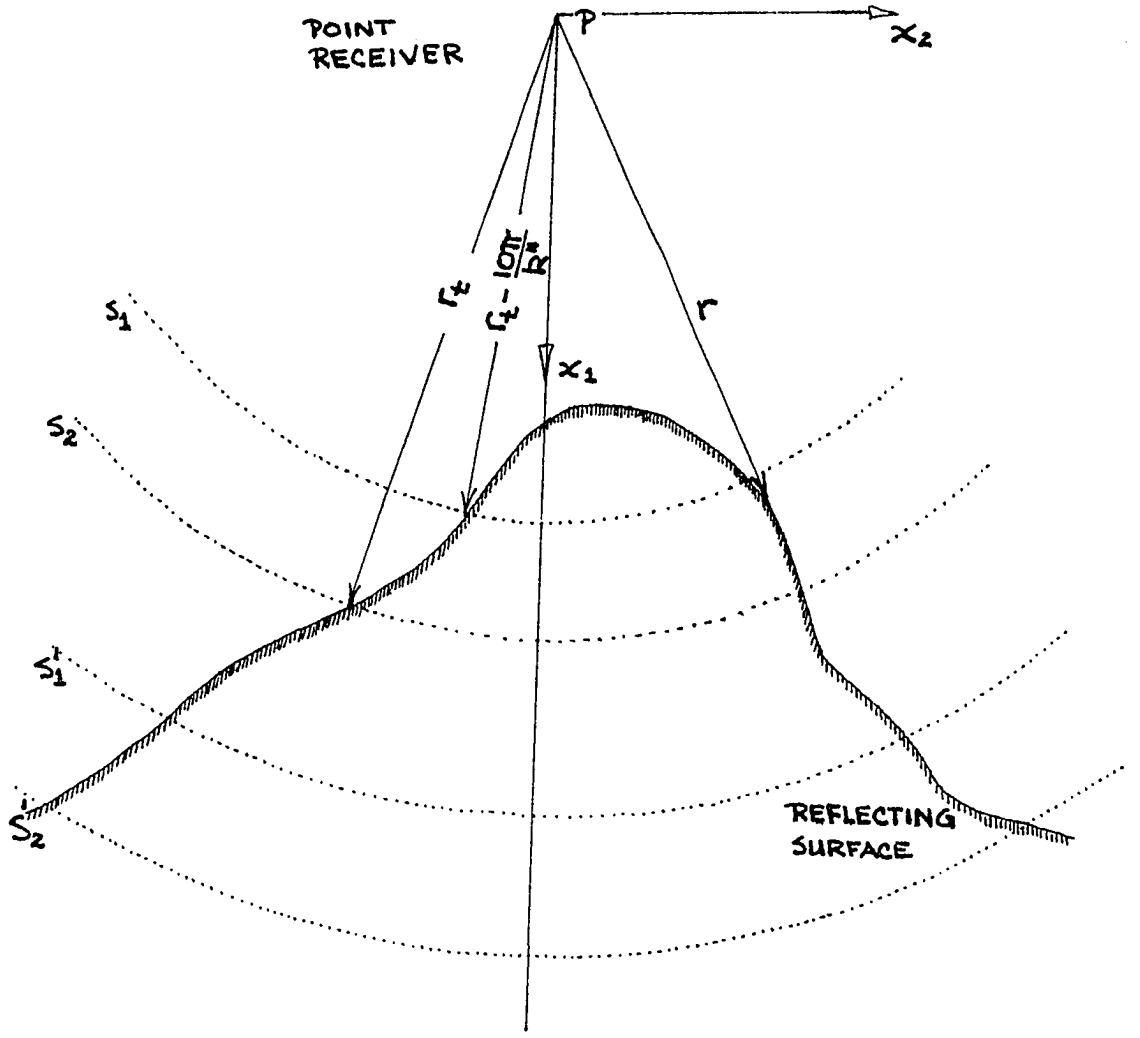

Figure 6. Limits on range of r during surface integration.

only yields the velocity potential at a point. The introduction of a finite receiver element as opposed to a point receiver will require a spatial summation or integration of the velocity potential over the face of the receiver element.

CHAPTER V. SIMULATION OF PULSE-ULTRASOUND SYSTEMS

The pulse reflection integral given at the end of Chapter IV still lacks sufficient generality to model finite size receiver elements. The problem could be remedied by deriving the reflection integral as a general function of r and then integrating the velocity potential over the surface of the receiver element. This approach leads to a fourth-order integral that would have to be evaluated for every value of t for which a solution is required. Another approach, which is more amenable to numerical methods, is to perform a translation of axis with respect to the reflecting surface. This allows a calculation of the velocity potential at different points in space and permits the modeling of the receiver surface as a finite number of point receivers. However, this results in four orders of numerical integration to be performed every time the value of t is changed. These computational requirements make such an approach highly undesirable in modeling a pulsed ultrasound system. In terms of the information derived, it would not appear to be cost effective for a designer or user of such systems to implement this type of algorithm to simulate the operation of their system.

Simplification is obviously desirable and can be made only with a loss of information and or accuracy. A decision on how much information or accuracy loss can be tolerated before an approximation becomes unacceptable is, as always, an engineering question which must be answered on a case by case basis. Typically, it appears that the information of greatest interest to users of pulsed ultrasound system is related to the relative magnitudes of the pulses appearing in an A-scan and their

approximate duration. In addition, knowledge of these two parameters as a function of lateral translation and angular rotation of the transducer with respect to the surface is also desirable.

The techniques introduced in this chapter are aimed at obtaining this information, in an approximate sense, with a technique that is both economical and relatively simple to use and should yield results of sufficient accuracy for general design work.

Thus, the chapter will begin with the development of such an algorithm and proceed to incorporate it into a model for a pulsed ultrasound system. The chapter will then conclude with an application of this model to a particular surface and compare the results with experimentally derived results.

Reflection Algorithm

In this initial investigation, it will be assumed that the surface always possesses one plane of symmetry. This assumption will reduce the computational complexity while still allowing a test of the validity of the approach.

The type of system which will be modeled in this work has a transducer with a single piezoelectric element which functions as both a transmitter and receiver of ultrasonic waves; this element will be viewed as being composed of m times n points. It will produce a beam which irradiates a segment of the reflecting boundary that will also be viewed as being composed of m times n elements. A segment on the reflecting surface will be designated by the values of the symbols p and q, while a segment

of the receiver will be designated by values of i and y. An example of this system for designating differential elements of the receiver and differential elements on the reflecting surface is given in Figure 7. It will be seen shortly that the introduction of this notation is a key element in using the pulse reflection integral to solve the type of pulse reflection problem depicted in Figure 7.

The pulse reflection integral, as presented in Chapter IV, calculates the velocity potential at a fixed point. Conceptually, if each differential receiver element is viewed as a point, then the integral can be applied i•y times to compute the signal received by each point on the surface. The total received signal can then be viewed as a function of the sum of these individual returns.

In order to calculate the pulse reflection integral at a particular point in space, using equation (4.44), it is necessary that all values used in the integral be stated with reference to a coordinate system located at that point. For example, referring to Figure 7, it is obvious that the distance to the element marked 4,4 on the reflecting surface is dependent upon the element on the receiver surface for which the velocity potential is being calculated. This type of dependency for the value of r is designated by using the symbol r(i,y,p,q), which simply means that one has to know which receiver element and which reflector element is being talked about before one can determine a value for r. Although the use of this type of symbolism does tend to complicate the appearance of any equation in which it is used, it does clarify the exact nature of the de-

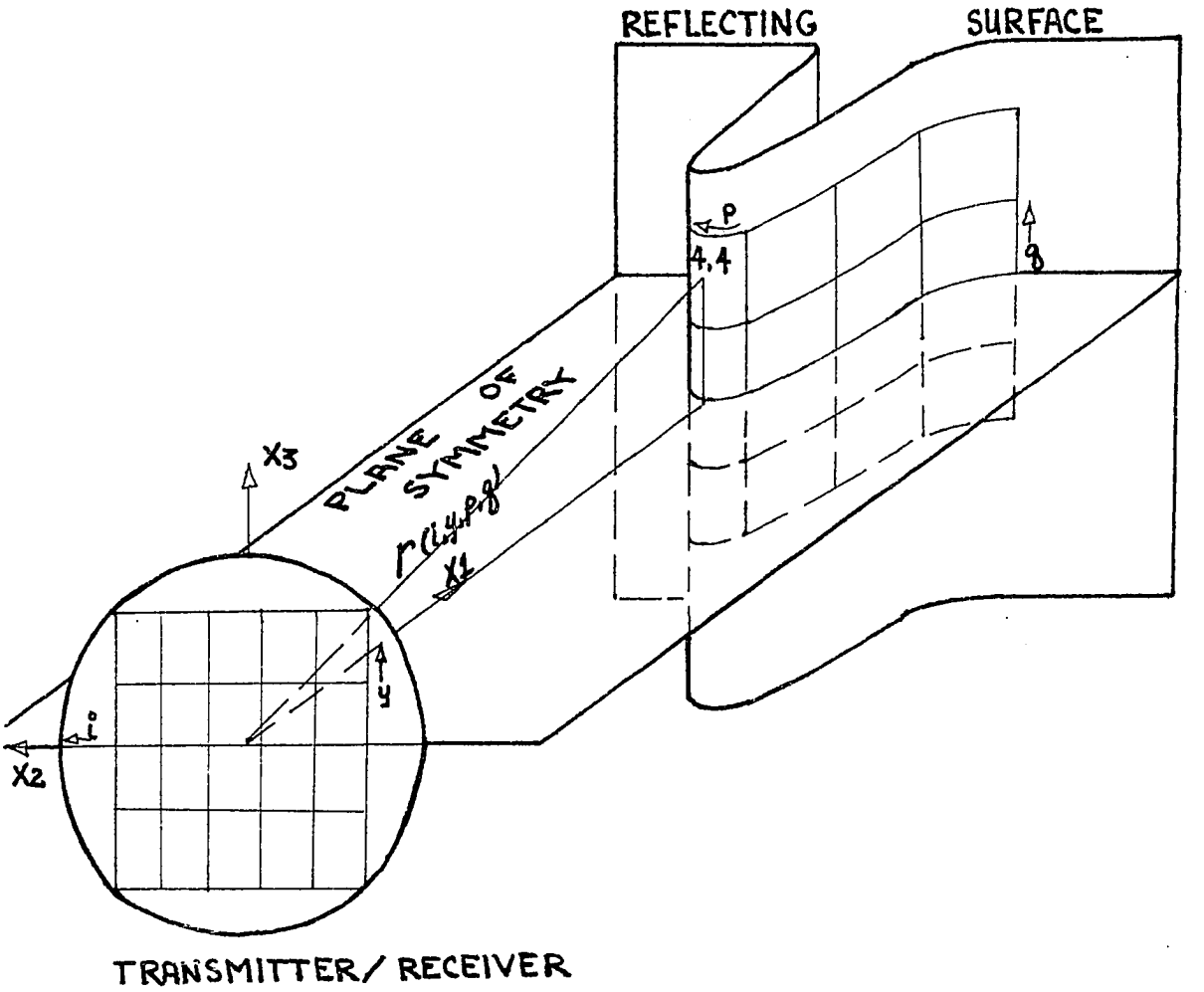

Figure 7. A specific source-surface reflection problem showing differential elements of transducer and reflector surface.

pendency of a particular variable and this clarification will serve to eliminate more confusion that it will cause.

With these thoughts on notation in mind, the pulse reflection integral of Chapter IV will now be expressed in a summation formula suitable for computer implementation. The formula emphasizes the relative location dependency of the different variables in addition to emphasizing the fact that the formula allows one to compute $\tilde{\phi}_R$ for a single differential element located at an arbitrary (i,y) position.

$$\tilde{\phi}_R(i,y,t) = \frac{1}{2\pi} \sum_{p=1}^{m} \sum_{q=1}^{n} \frac{R(p,q)V_I(p,q)}{r(i,y,p,q)} e^{jk(r_t - r(i,y,p,q))} \cos\alpha(p,q)\Delta s(p,q) \qquad (5.1)$$

There are several additional remarks that need to be made in reference to equation (5.1) to help clarify its meaning.

To begin with, the statement that V_I is a function of p and q might, at first, be a little perplexing. However, referring to the section on general considerations in Chapter IV it was stated that the incident field was going to be modeled as a particular type of plane wave whose amplitude would be allowed to vary from point to point on the wave front. The details of determining this empirically derived function will be discussed shortly but for the present it suffices to indicate that the amplitude of the incident wave can be referenced to a particular point on the reflecting surface. It should be pointed out that the location of the (p,q) element on the reflecting surface is dependent on the location of the transducer. Referring again to Figure 7, it can be seen that a lateral translation of the transducer would cause a different portion of

the reflecting surface to be irradiated and thus the (p,q) element would have a different location on the surface, in an absolute sense.

In a similar way, the reflection coefficient, R, and the cosine function, $\cos\alpha$, are both functions of p and q since the direction of the incident wave is independent of i and y. In the case at hand, the incident wave will be propagating in the x_1 direction and it is the angle between x_1 and the normal to the surface at a particular point that specifies a particular value for these two variables. Therefore, once the location of the transducer has specified the location of the p,q grid on the reflecting surface, these values can be computed independent of i and y.

Next, it can be seen that the area of the differential element, Δs, is also independent of i and y and thus it is shown as a function of p and q only.

The only variable left on the summation formula that actually proves to be a function of i, y, p and q is the distance r, the distance between a particular point source and a particular point receiver. The distance variable r_t is related to the range over which r can vary and is essentially a function of time. Of course, once the value of i and y are fixed r becomes a function of only p and q and then the summation formula has exactly the same physical interpretation as the pulse reflection integral of Chapter IV.

Before extending the present reflection formula to calculate the total receiver response, the variables r and r_t will be expressed in rectangular coordinates. This change will allow the introduction of

certain approximations that will simplify the calculation of the total response.

The variable r can be restated in the following terms,

$$r(i,y,p,q) = \frac{x_{1N}(p)}{\cos\gamma_{NP}(q,y)\cos\gamma_{TP}(i,p)} \tag{5.2}$$

where x_{1N} is defined as the distance from an element in the pth row to the plane of the transducer. Note that due to the symmetry of the reflecting surface this variable is constant with respect to variations in q and thus it is shown as a function of p only. The angle γ_{NP} in equation (5.2) is the angle between the line r(i,y,p,q) and the plane of symmetry. Referring to the example line shown in Figure 7, it can be seen that this angle is a function of q and y only. Next, the angle γ_{TP} is defined as the angle between the x_1 axis and a projection of r onto the plane of symmetry. In the example shown in Figure 7, this angle would be zero. In many cases of practical interest and in the specific problem to be considered later,

$$\cos\gamma_{NP}\cos\gamma_{TP} \approx 1 \tag{5.3}$$

which implies that

$$r = x_{1N}(p) \tag{5.4}$$

Using a similar development for r_t, it can be shown that

$$t = \frac{x_T}{c} \tag{5.5}$$

which implies that the limits on the exponential function can be stated as follows.

$$x_T - \frac{10\pi}{k''} \leq x_{1N} \leq x_T \tag{5.6}$$

In addition to these approximations for r and r_t, the presence of symmetry also allows some simplification of the variables R, cosα and ΔS. The variations in the values of R and cosα are both due to variations in the angle between the incident wave and the normal to the surface at a particular point. Since the incident wave is always propagating in the x_1 direction and the normal to the surface is constant with respect to variations in q, these two variables are a function of just the value of p and not p and q. With these facts in mind, it can be seen that cosα(p) times ΔS can be interpreted as the projection of ΔS onto an x_2, x_3 plane; this idea was illustrated earlier in Figure 5. Thus

$$\cos\alpha(p)\Delta S = \Delta x_2(p)\Delta x_3(q) = \Delta S'$$

where ΔS' is the projection of ΔS onto the x_2, x_3 plane.

These approximations can now be substituted into the reflection formula to yield the following equation.

$$\tilde{\phi}_R(i,y,t) = \frac{1}{2\pi} \sum_{p=1}^{m} \frac{R(p)}{x_{1N}(p)} e^{jk(x_T - x_{1N}(p))\Delta x_2(p)} \sum_{q=1}^{n} V_I(p,q)\Delta x_3 \qquad (5.7)$$

The summation over the q index will now be performed and a new variable B(p) defined.

$$B(p) = \sum_{q=1}^{n} V_I(p,q)\Delta x_3(q) \qquad (5.8)$$

This leads to an expression for $\tilde{\phi}_R$ in terms of the variable p.

$$\tilde{\phi}_R(i,y,t) = \frac{1}{2\pi} \sum_{p=1}^{m} \frac{R(p)B(p)}{x_{1N}(p)} e^{jk(x_T - x_{1N}(p))\Delta x_2(p)} \qquad (5.9)$$

It should be pointed out that the variable B(p) will prove to be the experimentally derived function describing the radiation characteristics

of a particular transducer. Its defining expression, given in equation (5.8), will be important in understanding exactly how these measurements should be made. The details of the measurements will be given in the next section, which will discuss the modeling of a particular pulsed-ultrasound system.

The expression for the velocity potential given in equation (5.9) now makes it a simple matter to calculate an approximation to the total response of the receiver in terms of a total velocity potential $\tilde{\phi}_T$. Since none of the terms in equation (5.9) are a function of i and y, a summation over these two indices leads to a simple multiplication of equation (5.9).

$$\tilde{\phi}_T(t) = \sum_{i=1}^{m} \sum_{y=1}^{n} \tilde{\phi}_R(i,y,t) = \frac{mn}{2\pi} \sum_{p=1}^{m} \frac{R(p)B(p)}{x_{1N}(p)} e^{jk(x_T - x_{1N}(p))} \Delta x_2(p) \qquad (5.10)$$

Equation (5.10) is in a form that admits to a relative simple physical interpretation which is helpful in understanding its implications and limitations.

Referring to Figure 8, the problem has been reduced to a single summation over a differentially wide strip of reflecting surface parallel to the plane of symmetry of Figure 7. In this particular illustration, the incident field can be viewed as being produced by a differentially wide transmitter strip where the magnitude of the incident wave is described by the function B(p). Recall that B(p) is actually a "weighted" value whose magnitude describes the sum of the incident wave amplitudes for all q elements located in the pth column. Therefore, the product of $B(p)R(p)\Delta x_2(p)$ describes the magnitude of a "weighted" point source

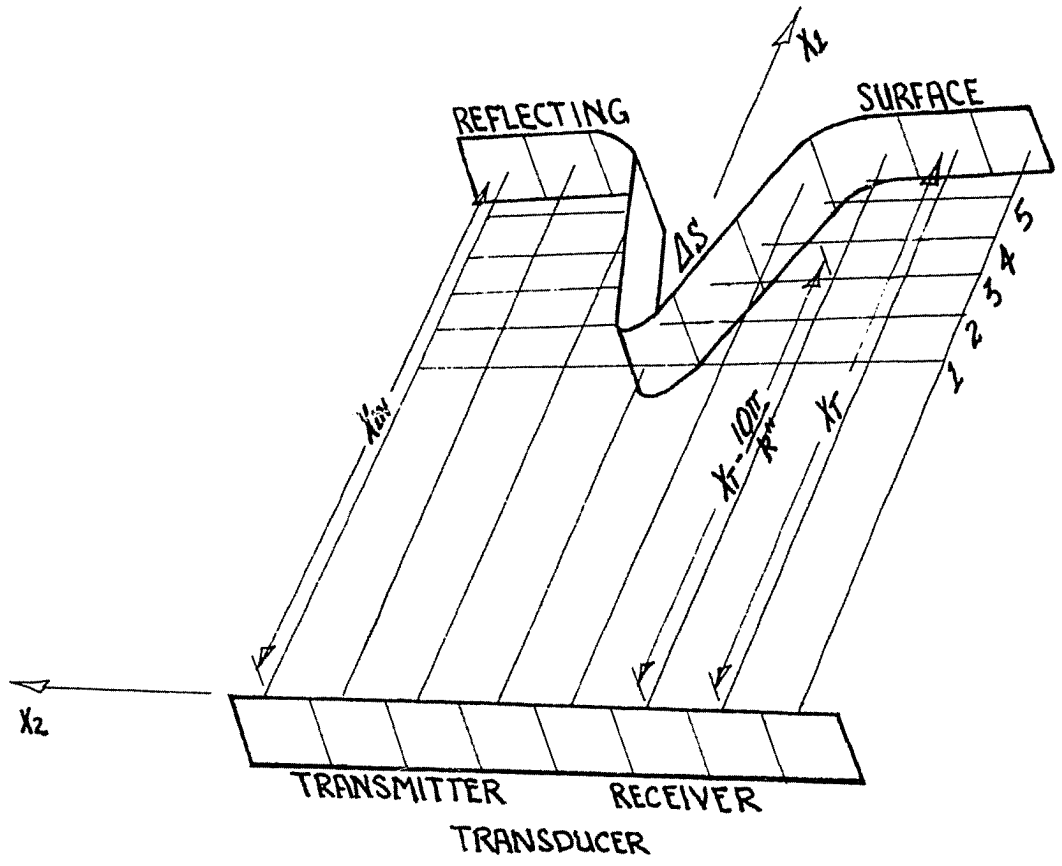

Figure 8. Source-surface reflection problem reduced to a differential strip.

located at the position of the particular differential element. Each one of these sources then radiates a signal which arrives at the plane of the transducer phase shifted and diminished in amplitude by an amount $e^{jk(x_T-x_{1n})}/x_{1N}$. It is the sum of each one of these contributions which provides an estimate of the total received signal, $\tilde{\phi}_T(t)$, at a particular instant of time. At a later time t, the value of x_T increases according to (5.5), and the limits on x_{1N} change according to (5.6). Thus the reflection formula is actually summed over a different part of the reflecting surface. These changes in the values of x_T and the range of x_{1N} show the time dependent nature of the reflection formula.

In summary, it can be said that the diameter of the transducer defines the limits on the value of x_2 while the duration of the radiated pulse and time defines the limits on the value of x_1 (i.e., x_T and $x_T - 10\pi/k''$). The source of the reflected wave is always located on the portions of the reflecting surface found within the range of these values.

As mentioned earlier, the reflection formula which has just been developed can be used to form the heart of an algorithm to simulate the operation of a pulsed-ultrasound system operating in the A-scan mode. The purpose of the next section is to develop such an algorithm for a particular system. The last section of this chapter will then compare results generated by the algorithm with experimental result obtained for a specific reflecting surface.

Ultrasound System Model

In order to facilitate this discussion on the development of a system model, a general block diagram of an A-scan system has been prepared and is presented in Figure 9. The development of a system model will consist in representing each one of the blocks with an appropriate expression and then linking these expressions together mathematically.

The representation of block one, the radiated field, has been discussed earlier. It amounts to the determination of an empirically derived function to represent the variable B(p). In the process of discussing the technique used to obtain B(p), a convenient method will be found to represent the entire system through block four.

An approach that is commonly taken to obtain information about the radiation patterns of a transducer involves the use of a small reflecting sphere. The sphere is located at a known point in the radiated field and is used to reflect a portion of the incident wave to a receiver element. The magnitude of the reflected wave is considered to be proportional to the magnitude of the incident wave at that point. An approach similar to this will be used to determine values of B(p). However, the defining expression for B(p), equation (5.8), represents a numerical line integral taken along a line normal to the plane of symmetry. This integral can be viewed as representing the strength of a line source. In order to approximate this situation experimentally, a long slender reflecting strip was used to reflect a signal proportional to B(p) back to the receiver. At the receiver, the signal was measured at the first convenient point; this point proved to be the output of the transducer (i.e., block 4, Figure 9).

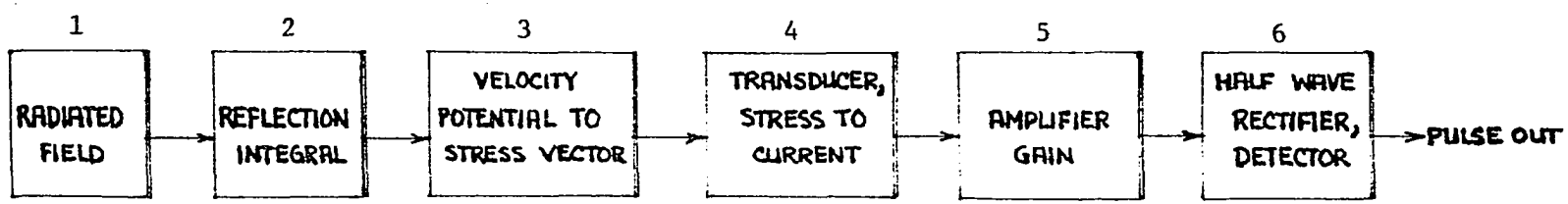

Figure 9. Block diagram of typical A-scan, pulsed-ultrasound system.

Thus, the signal as measured is a voltage that is related to B(p) through blocks two, three and four. That is, a narrow strip of the incident field is reflected back to the transducer and is converted from mechanical to electrical energy before being detected at the output of the transducer. There now remains the problem of showing how this electrical signal can be related to values of B(p).

Consider a situation in which a reflecting strip d units wide is being used to map the characteristics of the incident field. The strip is wide enough so that the reflection formula, equation (5.10), can be used but narrow enough to allow five or six measurements across the diameter of the field. The reflecting strip is made out of metal, while the propagating medium is water. This situation approximates a "perfect reflector" with a reflection coefficient of one being used in a "lossless medium," water. Since B(p) is a magnitude, the maximum value of the reflected wave is sought. After setting $\Delta x_2(p)$ equal to d and x_{1N} equal to x_s, the distance to the strip, equation (5.10) reduces to

$$|\tilde{\phi}_T| = \frac{mnd}{2\pi x_s} B(p) \tag{5.11}$$

where p now represents the position of the center of the strip. It is assumed that in general, $|\tilde{\phi}_T|$ can be related to the maximum value of the output voltage of the transducer by a constant of proportionality. This constant would represent the effects of blocks three and four, Figure 9. Letting $V_o(p)$ represent the transducer voltage as a function of the position of the strip, one can write

$$V_o(p) = H_T|\tilde{\phi}_T| = \frac{mnd}{2\pi x_s} H_T B(p) \tag{5.12}$$

where H_T is the transducer constant. Equation (5.12) can now be used in conjunction with (5.10) to develop a reflection formula that yields an answer in terms of transducer output voltage.

The constant H_T represents a general relationship between total velocity potential at the face of the transducer and transducer output voltage. Therefore, multiplying equation (5.10), the reflection formula, by H_T yields an expression for the output voltage of the transducer as a function of time. After multiplying (5.10) by H_T, equation (5.12) can be used to represent the quantity $H_T B(p)$ in terms of constants and the empirically derived function $V_o(p)$. This process leads to the following equation,

$$V_T(t) = \left| \frac{x_s}{d} \sum_{p=1}^{m} \frac{R(p)V_o(p)}{x_{1N}(p)} e^{jk(x_T - x_{1N}(p))} \Delta x_2(p) \right| \tag{5.13}$$

where $V_T(t)$ represents the output of block four, Figure 9.

The next step in the modeling process requires the representation of block five the amplifier gain. It will be assumed for the present that the amplifiers are a broadband design which does not change the shape of the pulse spectrum. It is, however, necessary to allow the gain to be a function of voltage since many pulsed-ultrasound systems use logarithmic amplifiers. For the present, the amplifier gain will be represented by a function G(v). This function would have to be determined experimentally for a particular system or in the case of design work it would be a design variable. An example of a nonlinear G(v) will be discussed in the next section on experimental results.

The final step necessary to complete the system model is to represent the half-wave rectifier and envelope detector of block six. Schematically, this block is represented by the circuit shown in Figure 10(a). The diode performs the half-wave rectification while the parallel RC network performs the envelope detection. The shape of the output pulse, P(t), is essentially determined by the magnitude of the returns and the RC time constant of the detector.

The input to this block is represented by the function $G(V_T(t))$ which is the results of equation (5.13) after being amplified. Since equation (5.13) is being evaluated on a digital computer, the output can be represented as a series of discrete values in time. This idea is represented by the solid lines in Figure 10(b), where the height of the lines represents the magnitude of the return at a particular instant in time. In the interval between these pulses, Δt, the shape of the pulse is determined by the RC time constant of the circuit.

The choice of a value for the RC time constant is somewhat arbitrary, but typically a value equal to the exponential damping on the radiated pulse is chosen. In this particular case then, an analog signal is obtained from the discrete values given by $G(V_T(t))$ by smoothing with a function of the form $e^{-w''t}$.

Application of Technique

In order to investigate the validity of the approach described in this work, an experiment was designed which would allow direct comparison

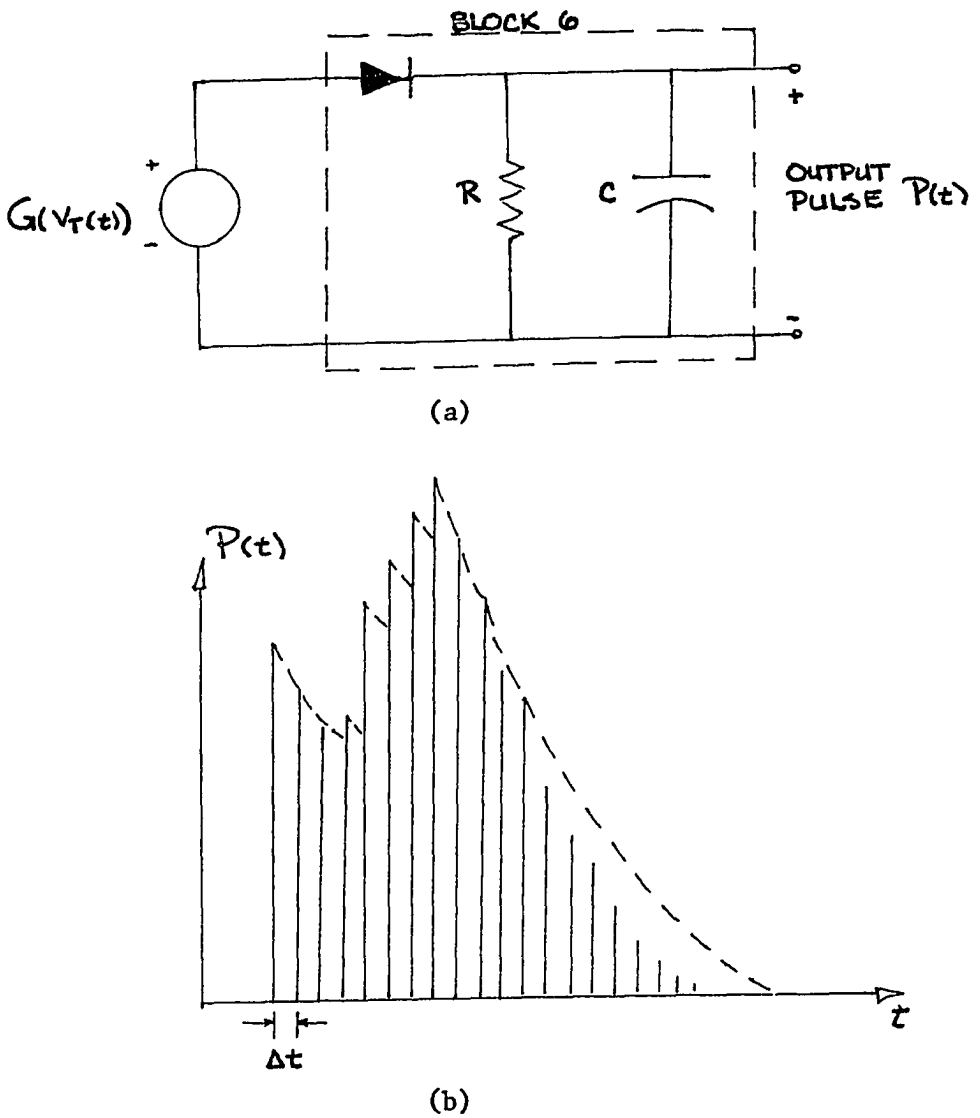

Figure 10. Rectification and envelope detection. (a) Half-wave rectifier and detector of A-scan pulsed-ultrasound system. (b) Representative output from block 6 generated by simulation program, showing specific pulses and corresponding envelope.

of experimentally measured and computer generated magnitude time plots of a particular system surface combination.

Overview

The experiment consisted of scanning the surface shown in Figure 11 with a pulsed ultrasound system connected to a Metrix PT50212 transducer with a crystal diameter of approximately 1.4 centimeters. The surface was made out of sheet aluminum approximately 1 millimeter thick and was immersed in a water bath at a distance of 12.58 centimeters from the face of the transducer at its closest point. The resonant frequency of the transducer is listed by the manufacturer as 2.25 megahertz. The output of the ultrasonic receiver was connected to a wideband oscilloscope to yield a magnitude versus time plot of the reflected pulses. These returns were then photographed at four different locations of the transducer with respect to the surface. The first return was for the transducer centered over the surface with the face of the transducer parallel to the base of the reflector. Subsequent photographs were made with the transducer laterally displaced with respect to the center point. The transducer was then returned to its center location and two additional photographs were made with the transducer rotated to two different angles.

After obtaining the experimental data the system was then used to obtain the information needed for the computer model. This consists of determining values for w", $V_o(p)$, and G(v).

A good approximation to w" can be obtained by observing the signal reflected off a plane reflector on an oscilloscope. This would be the signal before any nonlinear amplification, rectification and detection.

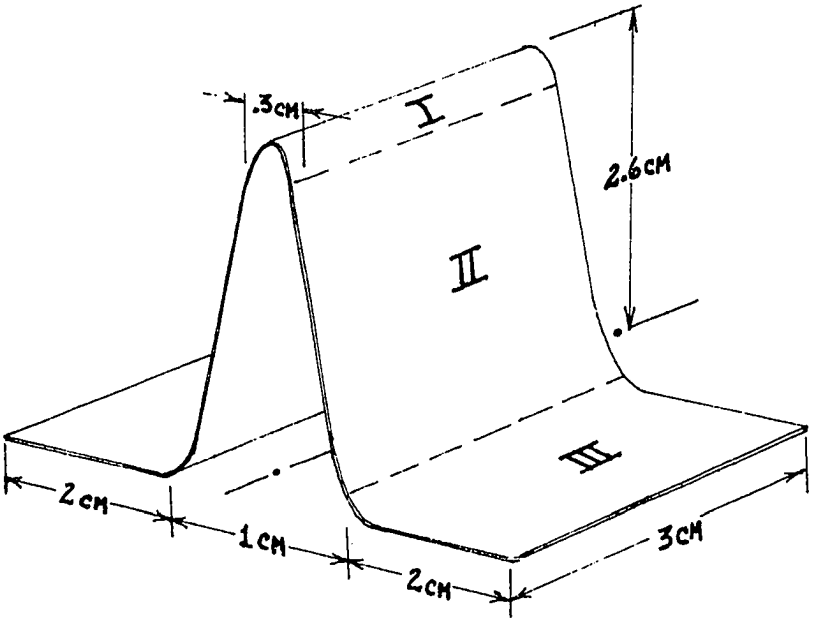

Figure 11. Perspective of trial surface with specific dimensions.

The signal is a reasonable facsimile of an exponentially damped sinusoid and a value for w" can be read directly off of the display.

Values for $V_o(p)$ were acquired using the technique discussed earlier and it was found, in this particular case, that the data could be quite accurately represented by an exponential function of p.

Finally, the transducer was disconnected from the receiver and the input driven by a variable amplitude sine wave generator at 2.25 megahertz while the output of the three stage amplifier section was monitored on an oscilloscope. Values for G(v) were then obtained and a piecewise fit of three different functions was finally arrived at as an adequate representation of the receiver gain characteristics.

The end results of all of the aforementioned measurements are listed in equation form below.

$$w'' = w'/2.22 \tag{5.14}$$

$$V_o(p) = 5.8687\, e^{-.0882302p} \tag{5.15}$$

$$G(v) = \begin{cases} 150v & v \leq .0400 \\ 11.5774v^{.1676091} & .0400 \quad v \leq .0750 \\ 8.0000v^{.0249158} & .0750 < v \end{cases} \tag{5.16}$$

All of the curve fitting was done on a Hewlett-Packard Model 67 calculator using their curve fitting program SD-03A.

The next step taken towards implementing the computer model was to fix the origin of the coordinate system and use three contiguous functions to describe the surface of Figure 10. Segment I was represented by a hyperbolic cylinder while segments II and III were represented by planes. It should be noted that this method was chosen as the most expedient way

of representing this particular surface, but it should not be construed that this is the only way or the most general way to represent an irregular surface. Equation (5.17) is the mathematical description of the reflecting surface used in the program.

$$f(x) = \begin{cases} .094378(x - .01583)^{1/2} & .1258 \leq x \leq .1268 \\ .10000x - .011180 & .1268 < x < .1518 \\ .1518 & x = .1518 \end{cases} \tag{5.17}$$

The final factor that needs evaluating before implementation of the computer algorithm is the reflection factor R. With the aluminum defined as region two and the water as region one values for the acoustic impedance are

$$z_2 = 17 \times 10^6 \text{ kg/m}^2\text{-sec}$$

$$z_1 = 1.5 \times 10^6 \text{ kg/m}^2\text{-sec}$$

These values were obtained from Table 1.1, page 14 of P. N. T. Wells' book Biomedical Ultrasonics (30). These numbers were substituted into equation (4.16) to obtain values of R for various angles of incidence and were stored as a table of values.

Computer program

A computer program was written to solve the radiation-reflection problem that has been described in this section. The program was optimized to solve this particular problem and no effort has been made to generalize it. Therefore, the only information that will be included here, with reference to the program, is a discussion of the approach taken

in solving the problem. This material is intended to serve as a starting point for anyone who might wish to write a general program.

Conceptually, the program can be broken into three parts. The first would involve the evaluation of equation (5.13), the reflection formula. The second would require using the value of V_T as an argument in G(v), equation (5.16), to determine the output from the amplifier section. And the third section would require calculating the effect of rectification and envelope detection.

The discussion begins with an explanation of the approach used in evaluating the reflection formula. This is best done with the aid of Figure 12. Figure 12 represents a cross section of the transducer and reflecting surface taken in the plane of symmetry. The shaded area represents the area occupied by the radiated pulse, which is propagating toward the surface with velocity c. At any instant of time the wave front is located at the position t/c, which is equal to x_T, and the trailing edge of the wave front is located at $x_T - 10\pi/k''$. It is obvious from the diagram that no reflected pulse is created for value of x_T less than x_c. Now let x_T equal x_c. In this case, the only nonzero contributions to $V_T(t)$ would be when x is equal to x_c. After summing over the p index, one would have the total reflected signal from that portion of the surface. This return will be designated as the return from position zero (RT(0)). Next increment the value of x_T to $x_c + \Delta x$. One could now sum all contributions from differential elements located at position x equal to $x_c + \Delta x$, called return at position one (RT(1)), plus all returns from elements at x equal to x_c. However, this later contribution was calcu-

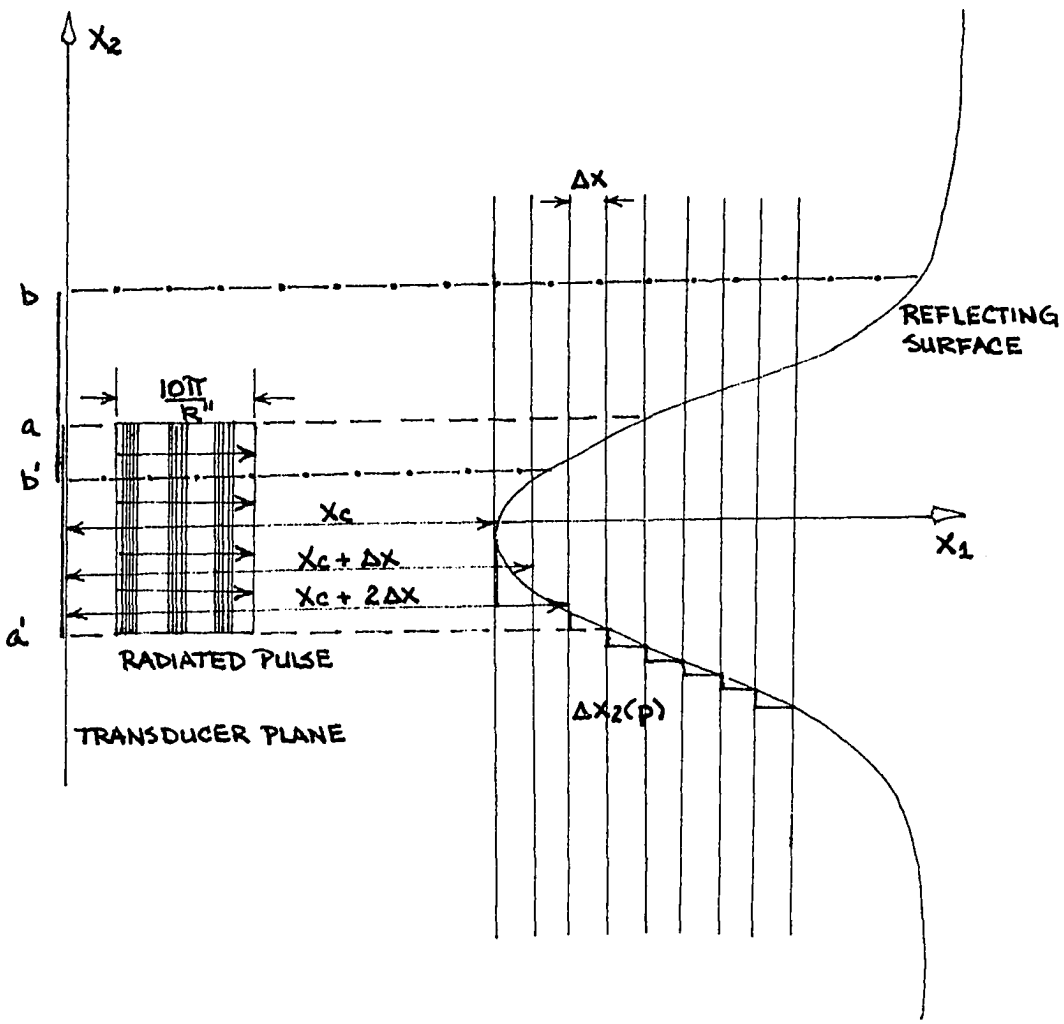

Figure 12. Cross section of reflecting surface and source showing variables associated with simulation program.

lated in the previous step as RT(0), the only difference is that the term needs to be multiplied by $e^{jk\Delta x}$. It is easy to see at this point that for x_T equal to $x_c + 2\Delta x$, the total return would be as follows.

$$V_T = RT(2) + RT(1)e^{jk\Delta x} + RT(0)e^{j2k\Delta x} \tag{5.18}$$

It follows that in the general case

$$V_T = RT(i)e^{jo} + RT(i - 1)e^{jk\Delta x} + RT(i - 2)e^{j2k\Delta x} + RT(i - 3)e^{j3k\Delta x} + \ldots \tag{5.19}$$

where the sum would continue until $nk''\Delta x$ was greater than $10\pi/k''$, where n is some integer. The value of i used in (5.19) would correspond to some position number and in some cases values for RT(i) may be zero. Thus, by using the circulating sum expression, equation (5.19), returns corresponding to certain distances from the source can be calculated and stored in a column matrix.

It can also be seen from Figure 12 that it is a relatively simple matter to simulate lateral translation of the source. In the example shown in the figure, the source has been moved from the position a - a' to b - b'. The effect of this translation is simply to define a different portion of the surface over which (5.13) must be evaluated. Such a translation often creates areas of overlap with segments of the surface that have been previously dealt with in other calculations. Thus in the interest of programming efficiency, it is helpful to separate the calculations into those that are dependent upon the position of the source and those that are not.

An examination of equation (5.13) and Figure 12 shows that the term $R(p)\Delta x_2(p)/x$ is independent of the lateral position of the source. This makes it convenient to calculate these terms only once for the entire surface and store them in a matrix along with their x_1, x_2 coordinates. Next the position of the source can be specified in terms of an upper and lower limit on the range of x_2. Once this is done, specific values of $V_o(p)$ can be matched with values of $R(p)\Delta x_2(p)/x$, multiplied together, and stored back in the matrix along with values of x_2 and x_1, the position of the differential element. This information can then be used with the circulating sum expression to obtain values of $V_T(t)$. The only constraint put on the sum expression is to make sure that the location of the differential elements are within acceptable limits on x_1 and x_2.

Once values of $V_T(t)$ are available, they can be used as the argument on the G(v) function to calculate the output of the amplifier section. Next, all negative values are replaced by zero to simulate half wave rectification. And finally, the specific values of output voltage can be plotted on a graph and the points fitted together with a function that simulates the effect of the envelope detector.

The description that has just been completed constitutes the basic program. There was a small modification that was added to it to simulate the effect of small angular rotation of the source around the x_3 axis.

The most pronounced change created by a small angular rotation of the source is to irradiate a different segment of the surface. This rotation was related to an equivalent translation which would cause the same segment of the surface to be irradiated. The appropriate values of $V_o(p)$ and

$R(p)\Delta x_2(p)x$ were then matched together. This constituted the description of the source for the reflected wave. However, the evaluation of $V_T(t)$ was conducted as if the transducer was in its original location. That is, the limits on x_2 were obtained by using the projection of the transducer onto the x_2, x_3 plane.

The method that has just been outlined serves as a basic overview of the computer simulation program. There are, however, some subtleties that one might wish to consider in writing a general program that are related to limitations of the physical optics approach. One of these limitations needs to be mentioned at this point, since it did play a part in writing the program used to generate the results of the next section.

It has been noted by several different authors that care must be taken in the physical optics approach when the angle of incidence becomes quite large. Meecham (28) points this out in his paper on the validity of the physical optics approach by noting that this condition can occur when determining the wave reflected off an irregular surface. It is stated that care must be exercised in retaining contributions to the reflected wave when the angle of incidence is large. Kouyoumjian (31) makes a similar point in his paper on asymptotic high-frequency methods. In a book entitled The Scattering of Electromagnetic Waves from Rough Surfaces, Beckmann and Spizzichino (27) also note the problem. They relate it to a concept discussed earlier in this chapter. From this point of view, it is stated that the surface needs to be rough, according to the Rayleigh Criterion, in order for the physical optics method to yield good results. As the angle of incidence increases the surface appears to be-

come smoother and the reflected energy tends to be radiated in the direction of specular reflection only. This idea is, of course, contrary to the physical optics implication that the energy radiates uniformly in all directions.

With this idea in mind it would seem prudent to ignore the return from a differential element if the angle of incidence becomes too large at that particular point. In fact this was done in the specific program used in this thesis work, by leaving out all returns from differential elements with an angle of incidence greater than eighty degrees. The choice of this particular value constituted an educated guess. The only method available for calculating such an angle requires the evaluation of the Rayleigh Criterion and the information needed to perform this calculation is very difficult to obtain.

The consideration of surface roughness completes the general discussion on all of the factors used in writing the computer program. The next section discusses the results obtained by applying this program in the specific situation described earlier.

Results

A comparison of the theoretical and experimental results shown in the next few figures should start by reviewing the objectives of the program. It should be remembered that the entire algorithm was optimized to produce computational simplicity and accurate prediction of a few essential parameters. These parameters are: position of the pulse in the A-scan plot, approximate pulse duration and magnitude information. With these thoughts in mind, the results essentially speak for themselves.

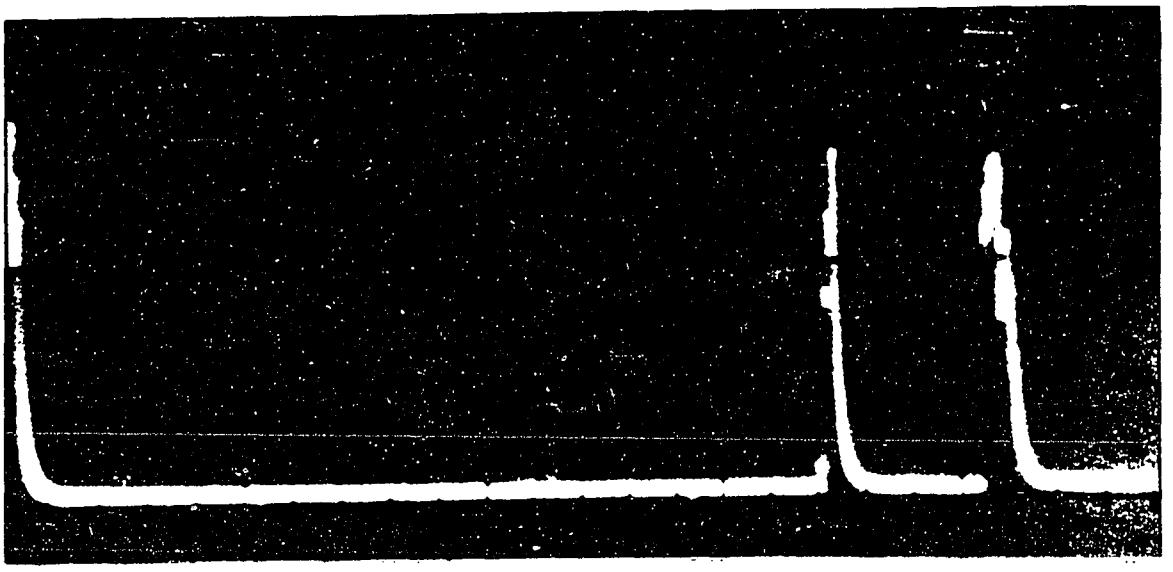

(a)

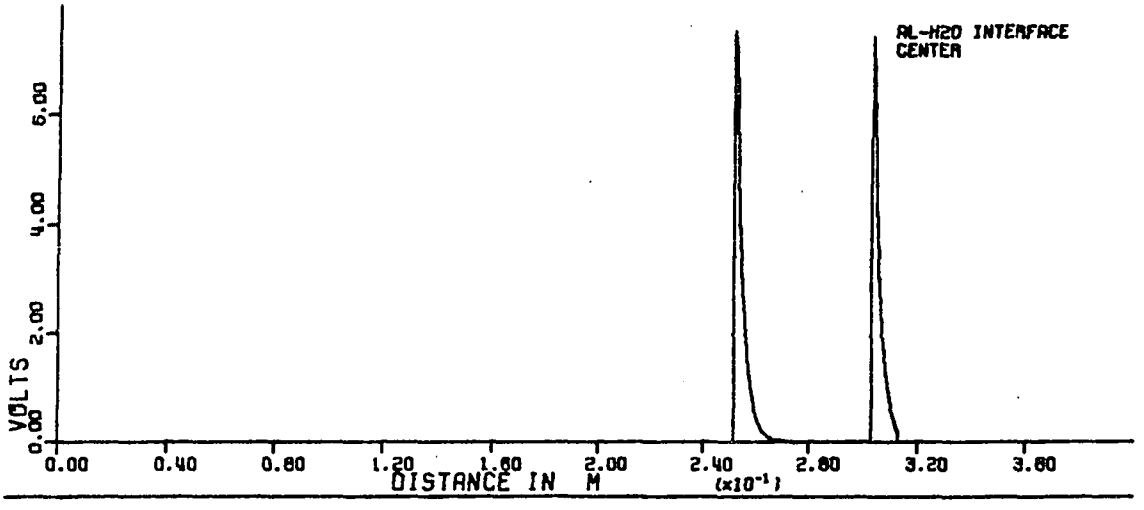

(b)

Figure 13. Output from pulsed-ultrasound system. (a) A-scan output for transducer centered over the surface shown in Figure 11 at a distance of 12.75 cm from the closest point. Horizontal axis calibrated at 7.5 cm/div., vertical axis calibrated at 5 v/div. (b) Corresponding computer plot for predicted A-scan output.

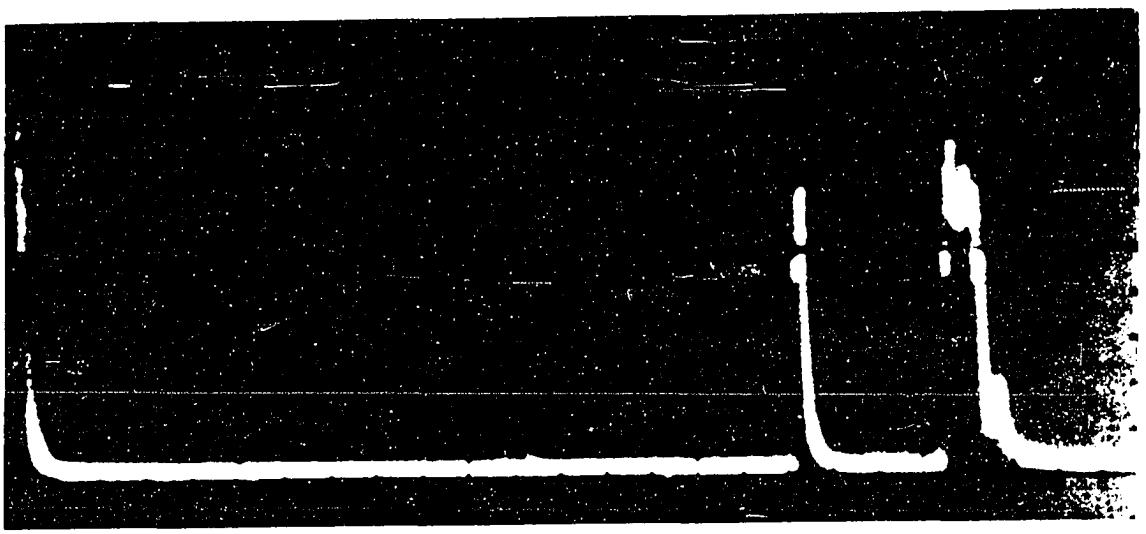

(a)

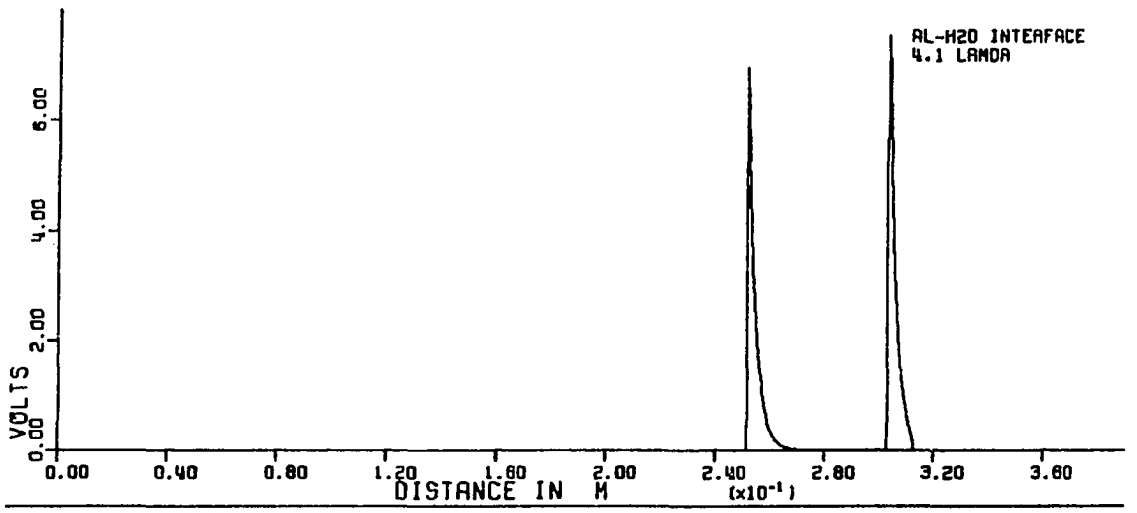

(b)

Figure 14. Output from pulsed-ultrasound system. (a) A-scan output with transducer laterally displaced .275 cm from position indicated in Figure 13. Calibration same as Figure 13. (b) Corresponding computer plot for predicted A-scan output.

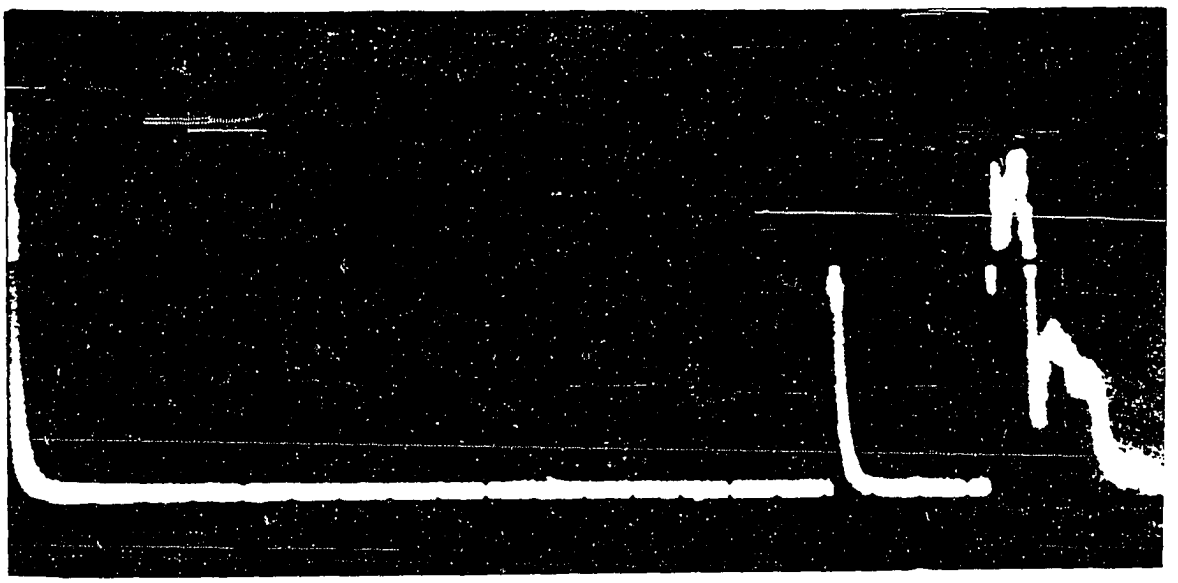

(a)

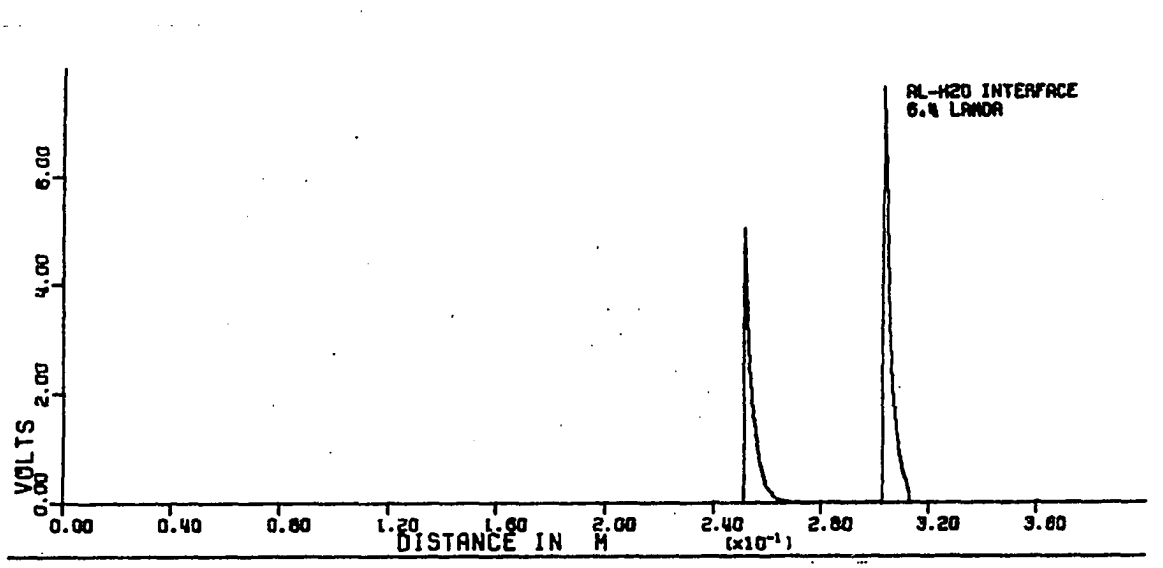

(b)

Figure 15. Output from pulsed-ultrasound system. (a) A-scan output with transducer laterally displaced .430 cm from position indicated in Figure 13. Calibration same as Figure 13. (b) Corresponding computer plot for predicted A-scan output.

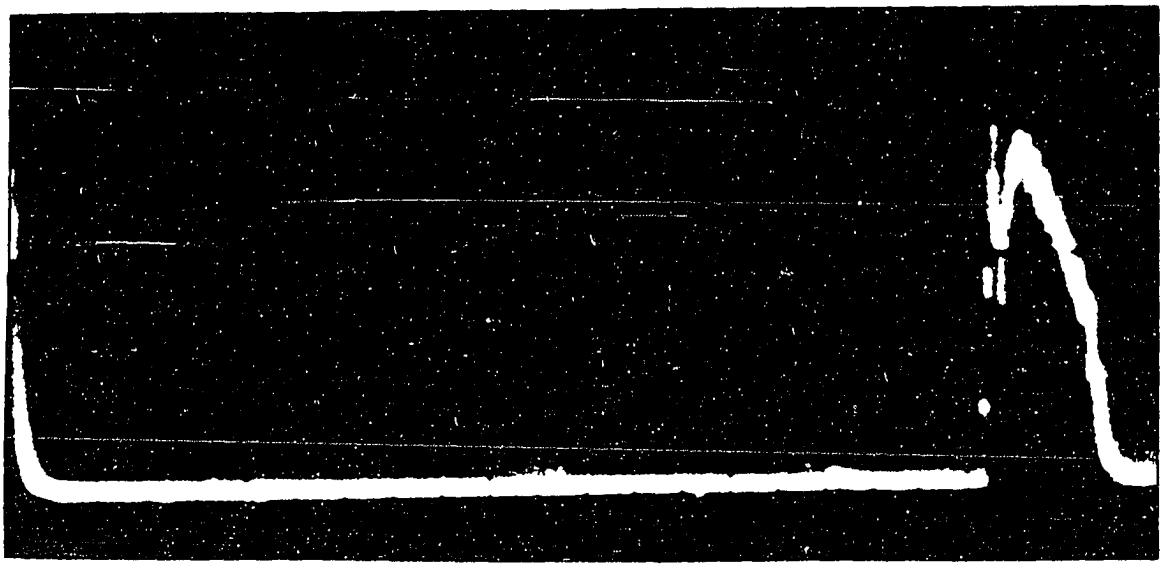

(a)

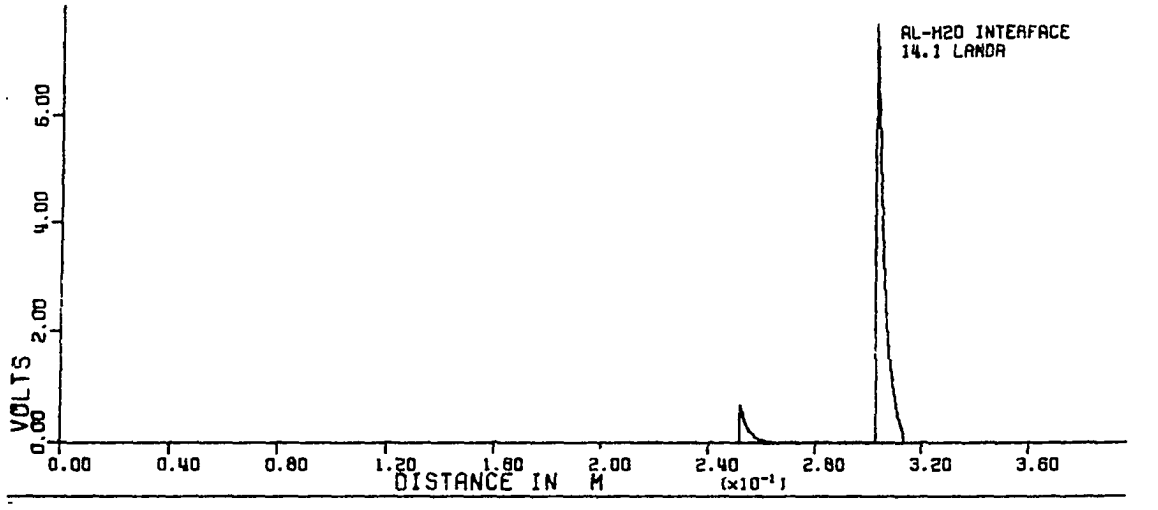

(b)

Figure 16. Output from pulsed-ultrasound system. (a) A-scan output with transducer laterally displaced .948 cm from position indicated in Figure 13. Calibration same as Figure 13. (b) Corresponding computer plot for predicted A-scan output.

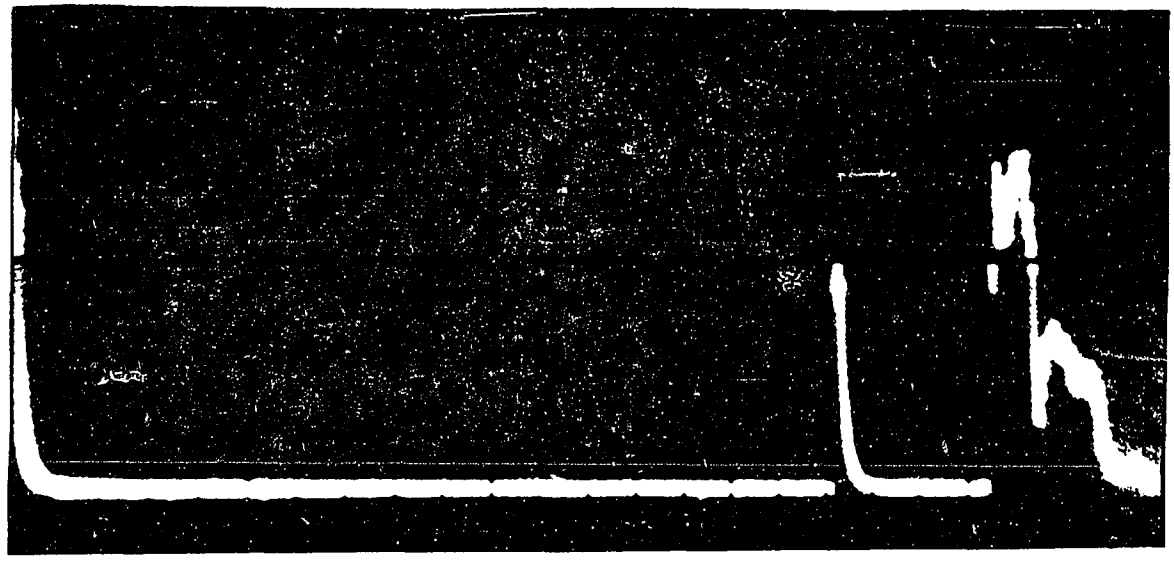

(a)

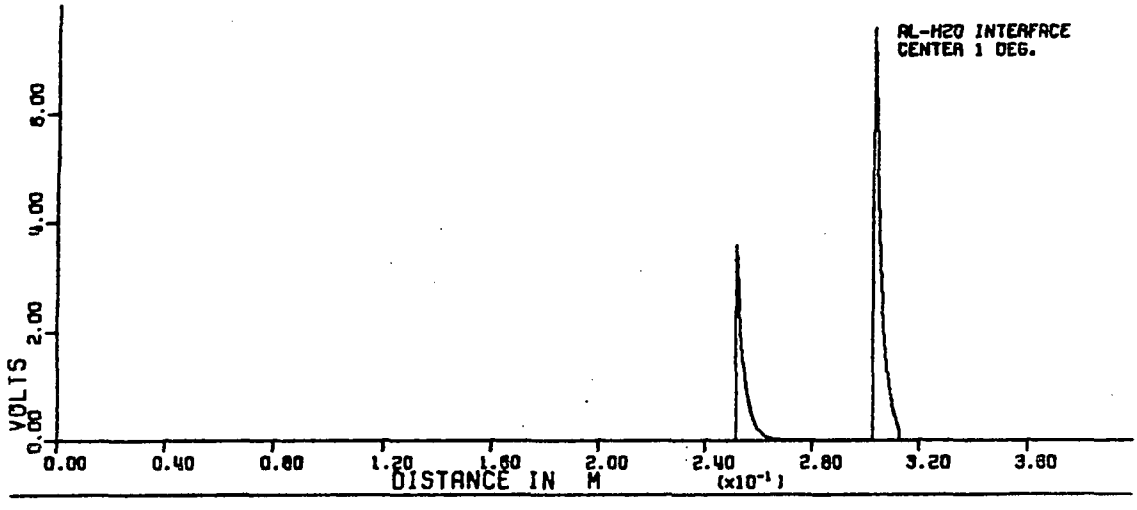

(b)

Figure 17. Output from pulsed-ultrasound system. (a) A-scan output with transducer centered over the surface at a distance of 12.75 cm from the closest point. Transducer mounted at the end of a mechanical arm 10.8 cm long and arm rotated 1 degree about x_3 axis. Calibration same as Figure 13. (b) Corresponding computer plot.

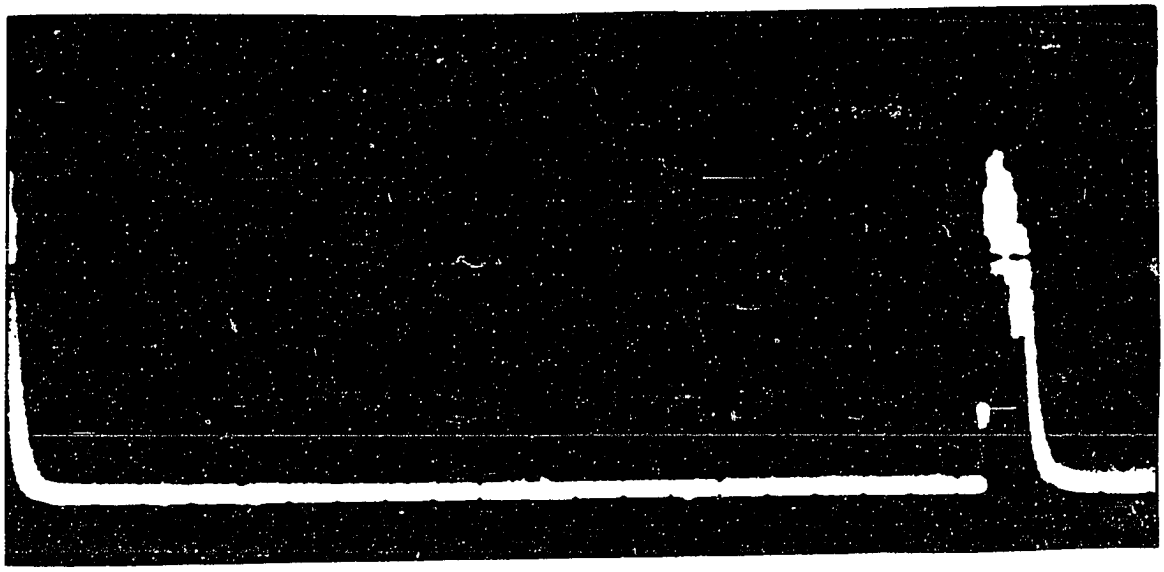

(a)

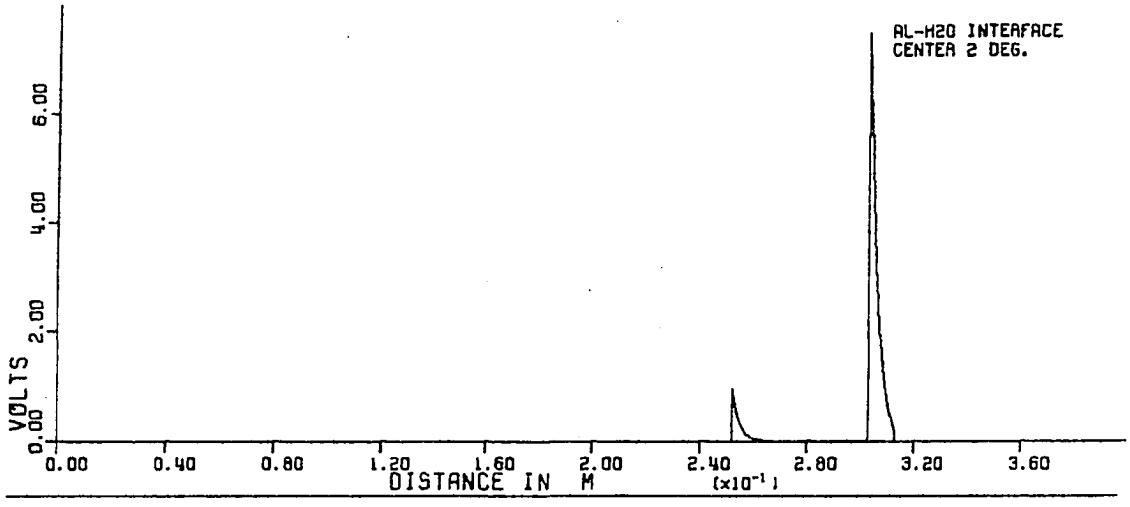

(b)

Figure 18. Output from pulsed-ultrasound system. (a) A-scan output with transducer rotated 2 degrees; otherwise conditions identical to Figure 17. (b) Corresponding computer plot.

Referring to the experimental results in Figure 13, the distance to the first pulse can be estimated from the assumed propagation velocity of 1500 m/sec and the sweep rate of 50 μ/sec per division. This yields a value of 25.5 cm shown on the computer plot. The pulse width in the experimental results are approximately 1.5 cm for the left hand or lead pulse and 1.8 cm for the right hand or trailing pulse. These values compare quite well with the computer generated values of 1.6 cm. However, a comparison of these values on subsequent figures shows a steadily increasing error for the trailing pulse. The source of this error is thought to be related to the tendency the amplifier section displayed to oscillate when subject to large signal inputs. This condition arose because the particular system used was designed to operate in a very lossy medium such as tissue, instead of water, which has very low losses. This explanation would account for the increase in pulse duration and for the trailing pulse as the transducer is shifted laterally. This shift results in larger signals being returned from the base of the reflecting surface and thus a more sustained oscillation. This increase in magnitude does not really show itself in the experiment or in the computer results due to the logarithmic nature of the amplifier gain.

The magnitude results, on the other hand, show far better agreement in general. The calibration for the vertical axis on the experimental results is 5 volts/div. Thus it can be seen that the computer generated values are always within a couple of tenths of a volt of the experimental values. The maximum error occurred for two degrees of angular rotation and amounts to about four-tenths of a volt.

In general, it can be said that the results from this particular application of the algorithm shows considerable promise for the simulation of A-scan systems in a more general environment. There does remain, however, a considerable amount of experimental work to be done before complete confidence in the technique would be warranted.

CHAPTER VI. CONCLUSIONS AND RECOMMENDATIONS

It is appropriate, at this point, to review the theoretical and empirical results presented in this thesis in light of the goals set forth in the introduction.

The introduction stated that the main objective of the thesis was the development of an analytical technique to simulate the operation of an A-scan, pulsed-ultrasound system. Subsequent statements elaborated on the idea by specifying model parameters for the simulation technique. It was stated that the technique should be computationally simple, capable of simulating lateral translation or small angular rotation of the transducer and be applicable to problems involving an irregularly shaped reflecting surface. These requirements precipitated an additional problem. The key to simulating a pulsed-ultrasound system is solving the inherent pulse reflection problem. However, the desired characteristics for the simulation technique ruled out the use of any existing pulse reflection algorithm. Thus, the stated objective for the thesis required the development of a new pulse reflection algorithm before the simulation problem could be addressed per se. For this reason, it seems appropriate to discuss the conclusions related to the pulse reflection algorithm somewhat apart from the simulation program, even though the former is an integral part of the latter.

The pulse reflection formula, in its most general form, is given in equation (4.44). The evaluation of this formula, for a specific r_t yields a value for the velocity potential of the reflected wave at a single point in space and time. The formula can be conveniently used to

handle a wide variety of pulse reflection problems, providing that the pulse shape can be described as an exponentially damped sinusoid. However, the author believes that the basic idea behind the development of (4.44) could be expanded to virtually any pulse shape that might arise in a physical situation. Such a generalization of the technique would probably be done most easily using a Green's function approach to formulate the reflection integral. The pulse reflection formula or any generalization of it is inherently capable of yielding an "exact" description of the reflected pulse. This point needs to be emphasized because the computational form of the formula was an approximate evaluation, optimized for pulse magnitude and duration not pulse shape. This is a reasonable thing to do when modeling A-scan systems, but most pulse reflection problems require information about pulse shape and thus this inherent capability needs to be emphasized.

While it is important to realize the inherent capabilities of the pulse reflection formula it is also important to appreciate its limitations. The formula is a physical optics approach to the reflection problem. The physical optics approach, in itself, yields approximate solutions to boundary value problems involving certain types of differential equations. A complete discussion of the limitations of physical optics would be quite lengthy and is not appropriate at this point. It suffices to say that potential users of the techniques presented in this thesis would do well to acquaint themselves with some of the literature in this area. Some of the references listed at the end of this work could serve as a starting point in such an effort. Perhaps one of the most helpful

ideas to keep in mind when using any physical optics method can be found in a quote from Electromagetic and Acoustic Scattering by Simple Shapes (32).

> Physical optics is probably the most widely used method for estimating the scattering. It is particularly convenient for machine computation, and because of this, the recent years have seen a growing tendency to credit physical optics with an accuracy which is in no sense justifiable. It is, therefore, unfortunate that necessary and sufficient conditions for the validity of the method cannot be stated, and indeed, several of the most fruitful applications have been in circumstances where prior justification would be difficult.

In short, conclusions on the validity of any physical optics type equation must always be stated in somewhat of a tentative fashion. This is an especially good point to remember, as conclusions on the applicability of the simulation program are stated.

The application and experimental verification of the simulation program presented in this thesis should be viewed as the results of a preliminary investigation. Considerable time and effort was expended in developing the theory behind the simulation program and in writing the program itself. Additional time could be, and should be, spent in writing a general program as a prelude to more extensive experimental investigations. However, some initial work needed to be done to see if such additional effort seemed warranted.

One firm conclusion that can be drawn as the result of this thesis is that future experimental work is certainly warranted. The object of these experiments would be to establish limits on the types of reflection problems that can be solved using the techniques developed in this work. At present, the author believes that the simulation program, or a variation of it, can be used to solve virtually any reflection problem that

might be of interest. In addition, it is felt that this approach to solving the problem would be as expedient as any available. However, until further experimental work is done, these remarks must remain as a statement of opinion rather than fact.

As a first step in establishing experimental limits on the simulation program, the results presented in this thesis need to be reviewed to see what specific conclusions can be drawn. In order to facilitate this discussion, the conclusions will be categorized into one of three areas. That is to say, they will be based upon information related to surface shape and size, or distance between source and object, or nature of the material properties of the propagating and reflecting media. The discussion begins with a brief look at the reflecting surface.

One of the more important considerations in testing the simulation program is the choice of the reflecting object. It is difficult at best to choose a representative irregularly shaped object. In fact the choice of surface shape, in this case, was primarily dictated by external factors, factors related to the design of an A-scan ultrasound system not associated with this work. Nevertheless, the surface does incorporate many facets which are desirable in a preliminary investigation. Some of these facets are: (1) large variations in surface slope, (2) large variations in radius of curvature, (3) substantial variation in distance along the axis of propagation from the closest to the farthest point on the object, (4) relatively easy to describe mathematically. The key characteristics the surface did not include were: substantial areas of constant, moderately sloped surface and substantial areas of gently curved surface.

Thus, one could conclude that surfaces that possess the characteristics listed in points one through three above can be approached with some confidence.

In keeping with the theme of a preliminary investigation, the simulation program was tested with the object located at a "moderate" distance from the source. The choice of this distance yielded two substantial benefits. First, the distance assured that the magnitude of the incident wave could be described by a well-behaved function. Second, the distance allowed the approximation introduced in equation (5.3) to be used.

Equation (5.3) requires that the product of two cosine functions, $\cos\gamma_{NP}$ and $\cos\gamma_{TP}$, be approximately equal to one. The fulfillment of this requirement allowed a great reduction in the computational complexity of the program. In addition, all of the equations presented after (5.3) assume that this requirement is met. This means that a more complex version of the simulation program must be written before one is ready to use the theory at close range. It should be emphasized that this extension to closer ranges is a computational problem not a theoretical one. As a point of reference, a lower boundary on the product of the two cosine functions is calculated for the particular problem considered in this thesis. It was found that the value never went below 0.9881.

As mentioned earlier, the moderate distance was also advantageous in describing the magnitude of the incident field at various points across the beam diameter. In this particular case it led to a simple exponential expression. However, it is well known that this description becomes considerably more complex the closer one gets to the transducer face. The

picture also changes much more rapidly as a function of distances at these closer ranges. Nevertheless, there is no reason to believe that the necessary incident field description cannot be obtained. It would, however, require a slightly different, more sophisticated approach than the one used in this thesis to derive the description. Recommendations, along this line, will be made in the next section.

The types of materials used in the experimental work presented in the thesis were aluminum and water. This choice led to very high values for the reflection coefficient; the range was 0.8 to 1. There is no anticipated difficulty with the use of the program on boundaries that yield lower values for the reflection coefficient. There are, however, some difficulties that could arise if one uses equation (4.16) as an approximation to equation (4.23).

Equation (4.16) is a formula for the reflection coefficient when neither medium can support shear waves. Equation (4.23) is a formula for the reflection coefficient when both mediums can support shear waves. Unless the propagation velocity of the shear waves is many times smaller than the propagation velocity of the longitudinal waves, equation (4.23) should be used. Otherwise substantial error in predicting the magnitude of reflected pulses may occur.

Recommendations

All of the recommendations for future work essentially fall into one category, that of additional experimental work.

The object of these experiments would be the determination of limits on the types of reflection problems that can be successfully handled using the simulation program. This work would require the writing of a general computer program to handle the many different surfaces that might be used in the experiments. In addition, a fast and efficient method of obtaining a digitized description of the reflecting surface would be needed.

As mentioned earlier, a more accurate method of determining $V_o(p)$ is also needed. It is thought that this could be accomplished by using a reflecting circular cylinder. The radius of the cylinder could be chosen as small as necessary to achieve the lateral resolution needed. Since the solution for scattering off cylinders is readily available in closed form, and exact relationship between $V_o(p)$ and $B(p)$ could easily be established.

The three factors that have just been mentioned constitute a considerable amount of work, but are a necessary prelude to the start of extensive experimental work.

The choice of the surfaces used in the experiments should follow the guidelines laid out in the conclusions. That is, the emphasis should be on gently curved and moderately sloped surfaces.

The materials used in the propagating and reflecting medium should yield small values for the reflection coefficient at normal incidence. In addition, materials with appreciable shear velocities should also be sought. This would allow a study of the effect of using equation (4.16) when the materials involved would dictate the use of equation (4.23).

Summary

In summary, it is felt that a significant step forward has been made in developing a tractable technique for predicting pulses reflected off irregularly shaped objects and in modeling pulsed-ultrasound systems. The primary emphasis in the development has been on the prediction of pulse magnitude and duration. However, theoretical ground work has been laid for the development of algorithms to predict pulse shape as well as magnitude and duration.

REFERENCES

1. A. Freedman. "Acoustic Echo Formation." Acustica 12 (1962): 11-21.

2. A. Freedman. "The High Frequency Echo Structure of some Simple Body Shapes." Acustica 12 (1962): 61-70.

3. D. M. Johnson. "Model for Predicting the Reflection of Ultrasonic Pulses from a Body of Known Shape." The Journal of the Acoustical Society of America 59 (1976): 1319-1323.

4. W. G. Neubauer. "A Summation Formula for Use in Determining the Reflection from Irregular Bodies." The Journal of the Acoustical Society of America 35 (1963): 279-285.

5. I. D. Ivanov. "Reflection and Refraction of a Plane Pulse at an Interface between Liquid Media." Soviet Physics Acoustics 19 (1973): 73-75.

6. I. D. Ivanov. "Reflection of a Spherical Pulse from a Fluid-Fluid Interface." Soviet Physics Acoustics 19 (1974): 342-344.

7. I. D. Ivanov. "Reflection of a Spherical Pulse from a Liquid-Solid Interface." Soviet Physics Acoustics 21 (1975): 259-261.

8. I. D. Ivanov. "Reflection of a Unit Spherical Pulse from a Liquid-Solid Interface." Soviet Physical Acoustics 21 (1975): 343-346.

9. W. Abramowitz. "Phase Distortion of Reflected Sonar Pulses." The Journal of the Acoustical Society of America 36 (1964): 214-215.

10. D. H. Towne. "Pulse Shapes of Spherical Waves Reflected and Refracted at a Plane Surface Separating Two Homogeneous Fluids." The Journal of the Acoustical Society of America 44 (1968): 65-76.

11. D. H. Towne. "Pulse Shape of Totally Reflected Plane Waves as a Limiting Case of the Cagniard Solution for Spherical Waves." The Journal of the Acoustical Society of America 44 (1968): 77-83.

12. B. F. Cron and A. H. Nuttall. "Phase Distortion Caused by Bottom Reflection." The Journal of the Acoustical Society of America 37 (1965): 486-492.

13. L. R. B. Duykers. "Deformation of an Exponential Pulse with a Finite Rise Time in the Region of Total Reflection." The Journal of the Acoustical Society of America 37 (1965): 1052-1055.

14. F. G. Friedlander. "Diffraction of Pulses by a Circular Cylinder." Communications on Pure and Applied Mathematics 7 (1954): 705-732.

15. F. G. Friedlander. "On the Total Reflection of Plane Waves." Quarterly Journal of Mechanics and Applied Mathematics 1 (1948): 376-384.

16. R. Forghieri. "Scattering of Impulsive Sound Waves by a Rigid Cylinder." Meccanica 9 (1974): 70-74.

17. I. A. Metsaveer. "Echo Signal of a Finite Spherical Pulse from a Fluid Filled Spherical Shell." Applied Mathematics and Mechanics 40 (1976): 599-605.

18. A. J. Rudgers. "Acoustic Pulses Scattered by a Rigid Sphere Immersed in a Fluid." The Journal of the Acoustical Society of America 45 (1969): 900-910.

19. R. Hickling. "Analysis of Echoes from a Solid Elastic Sphere in Water." The Journal of the Acoustical Society of America 34 (1962): 1582-1592.

20. R. Hickling. "Analysis of Echoes from a Hollow Metallic Sphere in Water." The Journal of the Acoustical Society of America 36 (1964): 1124-1137.

21. W. Kaplan. Advanced Calculus, 2nd ed. London: Addison-Wesley, 1973.

22. E. Skudrzyk. The Foundations of Acoustics. New York: Springer-Verlag, 1971.

23. W. P. Mason. Physical Acoustics, Vol. 1, Pt. A. New York: Academic Press, 1964.

24. W. G. Cady. Piezoelectricity. New York: McGraw-Hill, 1946.

25. I. V. Misyurkeyev. Problems in Mathematical Physics. New York: McGraw-Hill, 1966.

26. W. P. Mason. Physical Acoustics and the Properties of Solids. New York: D. Van Nostrand Co., 1958.

27. P. Beckmann and A. Spizzichino. The Scattering of Electromagnetic Waves from Rough Surfaces. New York: Pergamon Press, 1963.

28. W. C. Meecham. "On the Use of the Kirchhoff Approximation for the solution of the Reflection Problems." Journal of Rational Mechanics Analysis 5 (1956): 323-333.

29. R. D. Ford. Introduction to Acoustics. Amsterdam: Elsevier Pub. Co. Ltd., 1970.

30. P. N. T. Wells. Biomedical Ultrasonics. New York: Academic Press, 1977.

31. R. G. Kouyoumjian. "Asymptotic High-Frequency Methods." Proceedings of the IEEE (August 1965): 864-879.

32. J. J. Bowman. Electromagnetic and Acoustic Scattering by Simple Shapes. Amsterdam: North Holland Pub. Co., 1969.

ACKNOWLEDGMENTS

I wish to express my appreciation to all the people who have helped me and supported me in this work, especially Dr. Post for his most valuable guidance in the theoretical aspects of this thesis and Dr. Carlson for his help in the design and construction of equipment used in the experimental work. I wish to especially thank my mother for her many years of support and encouragement and my lovely wife for her patience, love and understanding.